Supplementary Information

Comprehensive analysis of m6A-seq data reveals distinct features of conserved and unique m6A sites in mammals

Guo-Shi Chai[1,2], Hong-Xuan Chen[1,3], Dong-Zhao Ma[1], Ze-Hui Ren[1,3], Xue-Hong Liu[1], Zhang Zhang[1], Guan-Zheng Luo[1,3,4]*

[1]State Key Laboratory of Biocontrol, MOE Key Laboratory of Gene Function and Regulation, Guangdong Province Key Laboratory of Pharmaceutical Functional Genes, School of Life Sciences, Sun Yat-sen University, Guangzhou 510275, China

[2]Westlake Laboratory of Life Sciences and Biomedicine, Hangzhou, Zhejiang, China

[3]Sun Yat-sen University Institute of Advanced Studies Hong Kong, Science Park, Hong Kong SAR, 999077, China

[4]Innovation Center for Evolutionary Synthetic Biology, Sun Yat-sen University, Guangzhou 510275, China

* Correspondence to: luogzh5@mail.sysu.edu.cn

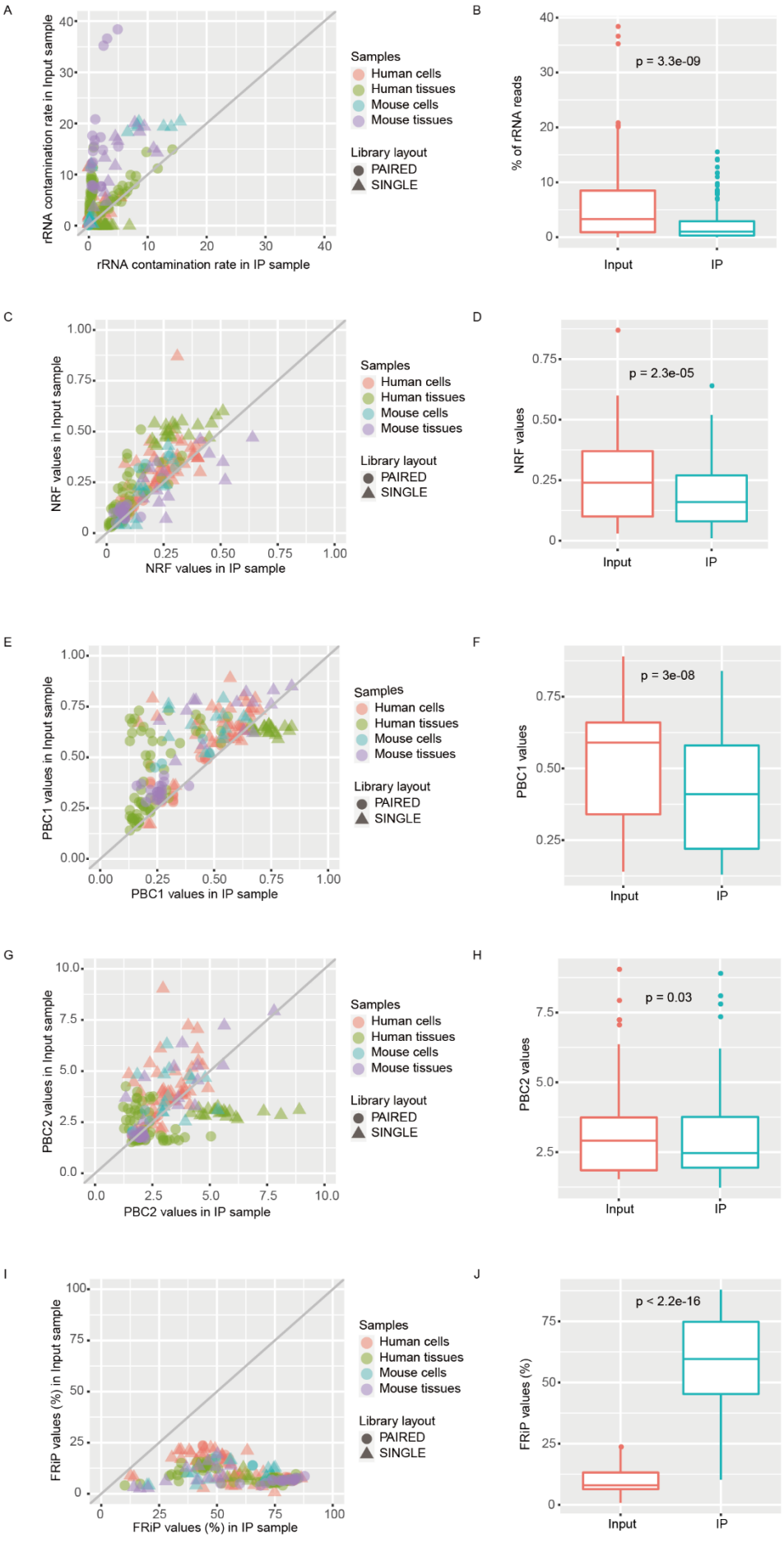
A
rRNA contamination rate in Input sample
rRNA contamination rate in IP sample
Samples
Human cells
Human tissues
Mouse cells
Mouse tissues
Library layout
PAIRED
SINGLE
B
% of rRNA reads
p = 3.3e-09
Input
IP
C
NRF values in Input sample
NRF values in IP sample
D
NRF values
p = 2.3e-05
E
PBC1 values in Input sample
PBC1 values in IP sample
F
PBC1 values
p = 3e-08
G
PBC2 values in Input sample
PBC2 values in IP sample
H
PBC2 values
p = 0.03
I
FRiP values (%) in Input sample
FRiP values (%) in IP sample
J
FRiP values (%)
p < 2.2e-16

Supplementary Figure 1 **Quality evaluation of 193 pairs of IP and input samples.** A, B, Distribution of rRNA contamination rates in IP and Input samples. C, D, Distribution of NRF values in IP and Input samples. E F, Distribution of PBC1 values in IP and Input samples. G, H, Distribution of PBC2 values in IP and Input samples. I, J, Distribution of FRiP values in IP and Input samples.

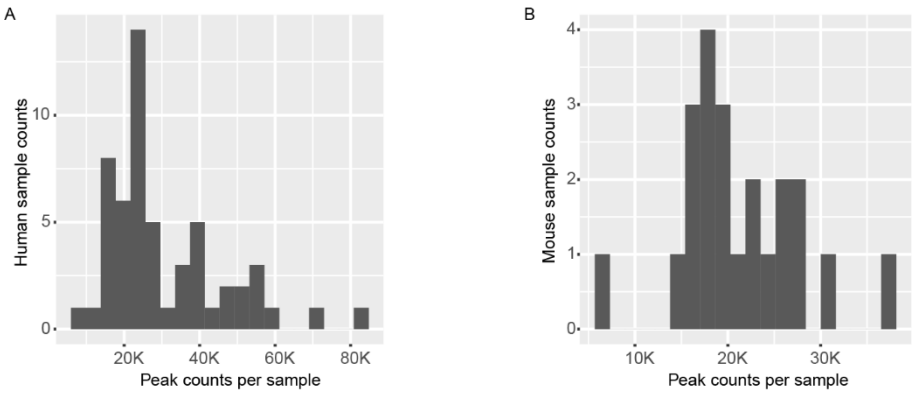

Supplementary Figure 2 **Number of detected m6A sites.** The number of m6A sites detected in human samples (A) and mouse samples (B).

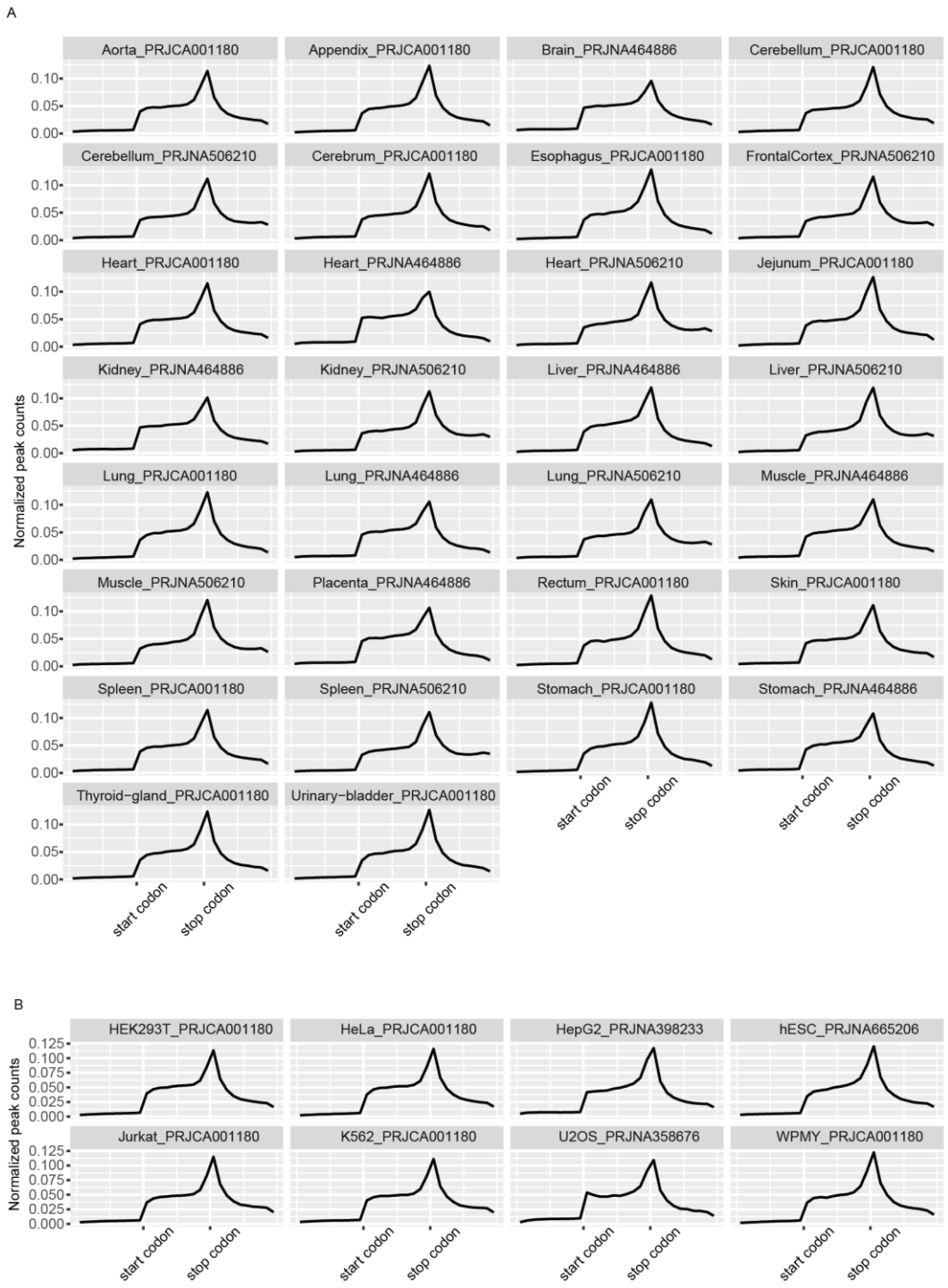

Supplementary Figure 3 **The distribution pattern of m6A sites on the transcriptome.** The distribution pattern of m6A sites in 30 human tissues (A) and 8 human cell lines (B). All of m6A sites in individual sample were used for metagene analysis for m6A site quality evaluation. Metagene profiles were generated using MetaPlotR, dividing the 5'-UTR, CDS, and 3'-UTR regions into 150 bins. The y-axis represents the normalized peak count, calculated as the number of m6A sites in each bin divided by the total number of m6A sites for the human tissue or cell line.

Supplementary Figure 4 **Consensus motif sequences significantly enriched at m6A sites.** Enriched motif sequences in 30 human tissues (A) and 8 human cell lines (B).

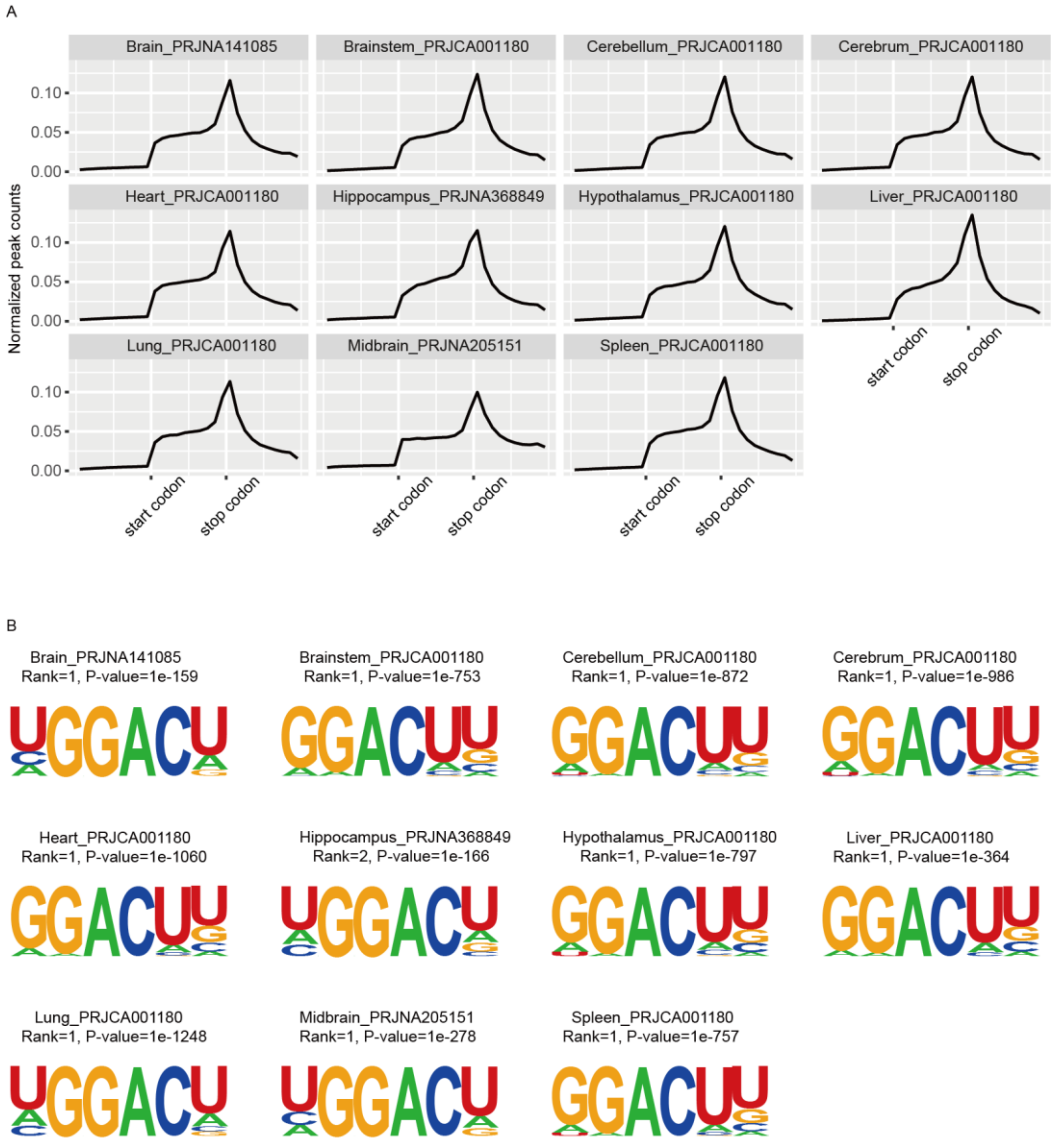

Supplementary Figure 5 A, The distribution pattern of m6A sites along the transcriptome for 11 mouse tissues. B, Consensus motif sequences significantly enriched at m6A sites for 11 mouse tissues. All of m6A sites in individual sample were used for metagene analysis for m6A site quality evaluation. Metagene profiles were generated using MetaPlotR, dividing the 5'-UTR, CDS, and 3'-UTR regions into 150 bins. The y-axis represents the normalized peak count, calculated as the number of m6A sites in each bin divided by the total number of m6A sites for the mouse tissue.

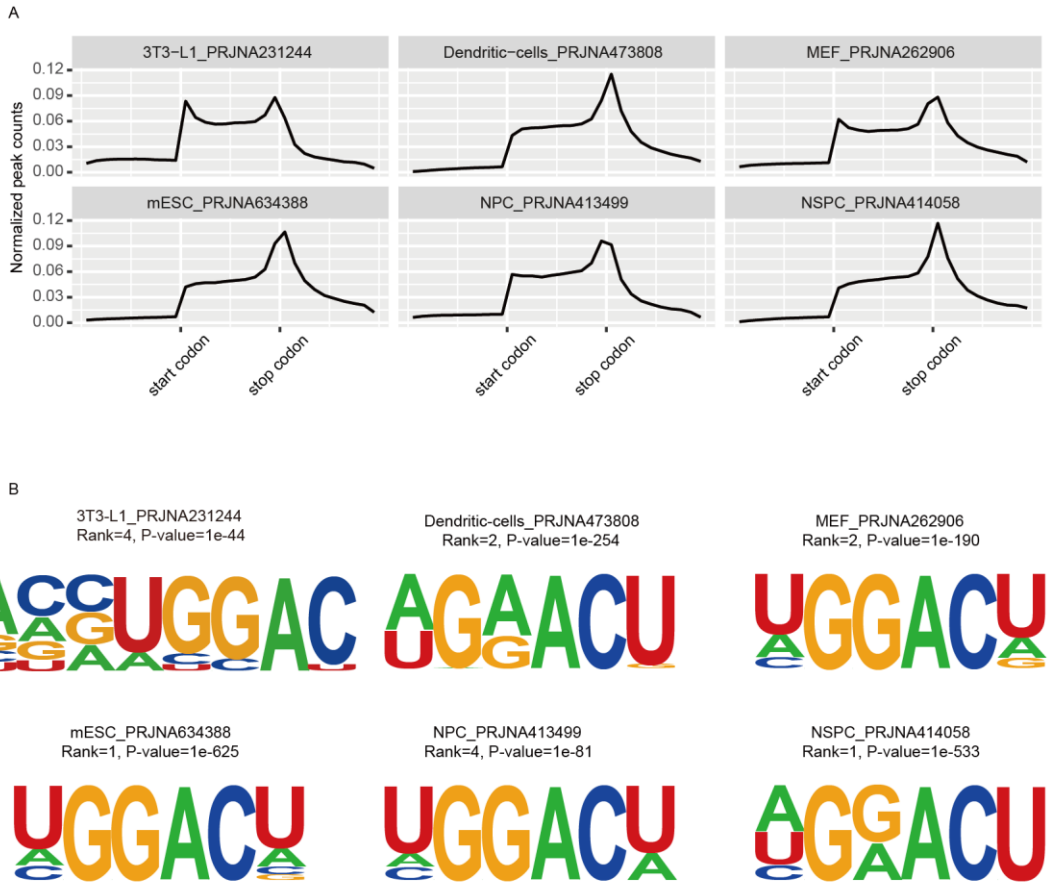

Supplementary Figure 6 A, The distribution pattern of m6A sites along the transcriptome for 6 mouse cell lines. B, Consensus motif sequences significantly enriched at m6A sites for 6 mouse cell lines. For 3T3-L1, the top 5,000 most significant m6A sites produced motif sequences with 100% adenine. For other samples, all of m6A sites were used to produced motif sequences. All of m6A sites in individual sample were used for metagene analysis for m6A site quality evaluation. Metagene profiles were generated using MetaPlotR, dividing the 5'-UTR, CDS, and 3'-UTR regions into 150 bins. The y-axis represents the normalized peak count, calculated as the number of m6A sites in each bin divided by the total number of m6A sites for the mouse cell line.

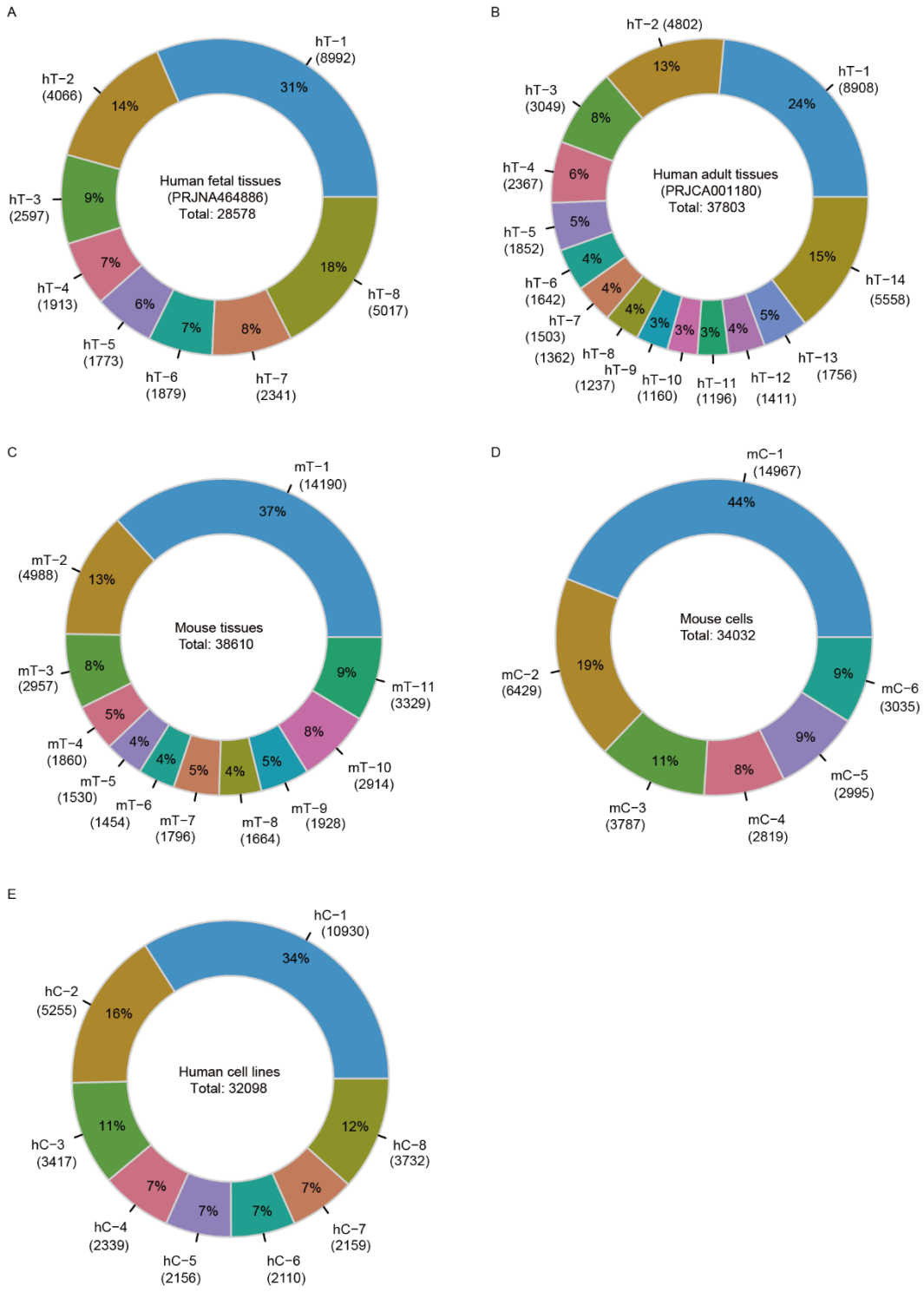

Supplementary Figure 7 **The number and proportion of m6A sites of different consistency levels in human tissues and cell lines, and mouse tissues and cell lines.** A, The m6A sites detected in eight different human fetal tissues are classified into eight consistency levels, and the number and proportion of m6A sites of eight consistency levels are shown. B, The m6A sites detected in fourteen different adult tissues are classified into fourteen consistency levels, and the number and proportion of m6A sites of fourteen consistency levels are shown. C, m6A sites detected in eleven different mouse tissues are

classified into eleven consistency levels, and the number and proportion of m6A sites of eleven consistency levels are shown. D, m6A sites detected in six different mouse cell lines are classified into six consistency levels, and the number and proportion of m6A sites of six consistency levels are shown. E, m6A sites detected in eight different human cell lines are classified into eight consistency levels, and the number and proportion of m6A sites of eight consistency levels are shown. hT denotes human tissue. hT-1 denotes that m6A is present in one type of human tissue. hT-8 denotes that m6A is present in eight different human tissues simultaneously. mT denotes mouse tissue. mT-1 denotes that m6A is present in one type of mouse tissue. mT-11 denotes that m6A is present in eleven different mouse tissues simultaneously.

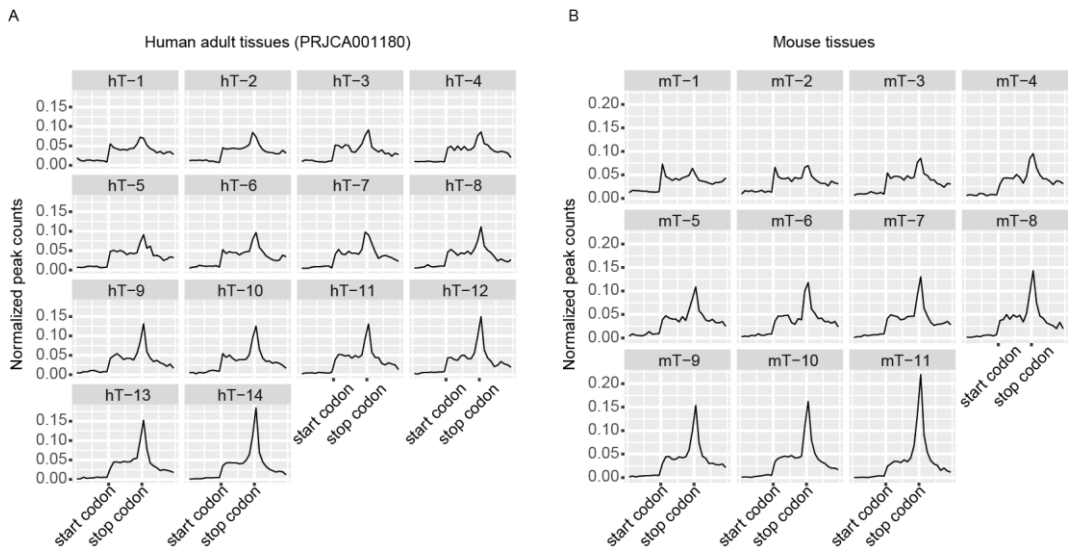

Supplementary Figure 8 **The distribution patterns of m6A sites with different consistency levels in human and mouse tissues.** A, Distribution patterns of m6A sites of fourteen consistency levels defined by fourteen different adult tissues along the transcriptome. B, Distribution patterns of m6A sites of eleven consistency levels defined by eleven different mouse tissues along the transcriptome. Metagene profiles were generated using MetaPlotR, dividing the 5'-UTR, CDS, and 3'-UTR regions into 150 bins. The y-axis represents the normalized peak count, calculated as the number of m6A sites in each bin divided by the total number of m6A sites for that consistency level. hT denotes human tissue. hT-1 denotes that m6A is present in one type of human tissue. hT-14 denotes that m6A is present in fourteen different human tissues simultaneously. mT denotes mouse tissue. mT-1 denotes that m6A is present in one type of mouse tissue. mT-11 denotes that m6A is present in eleven different mouse tissues simultaneously.

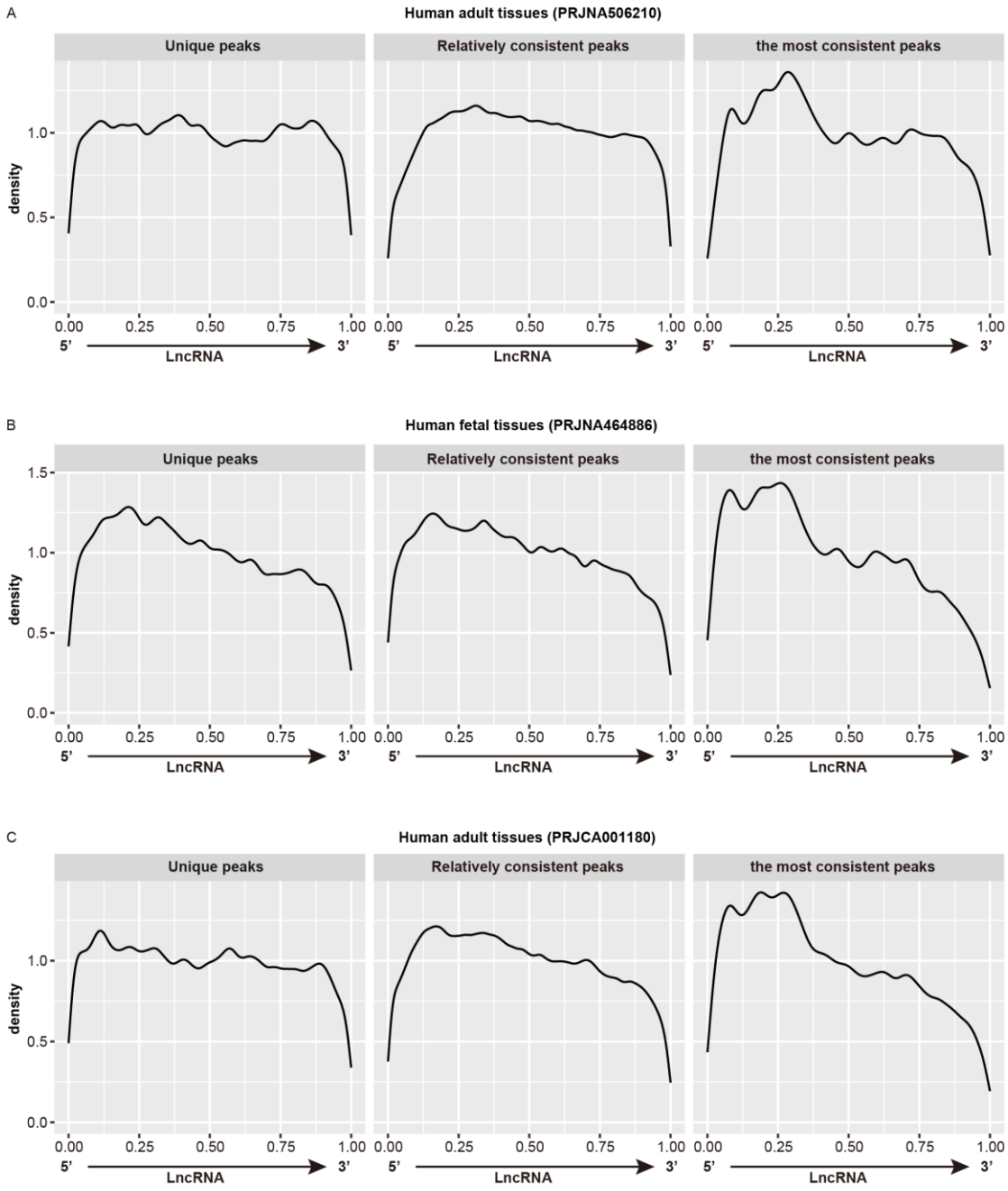

Supplementary Figure 9 The distribution patterns of m6A on lncRNA. The distribution of m6A sites with varying consistency levels on lncRNA across 8 adult tissues (A), 8 fetal tissues (B), and 14 adult tissues (C).

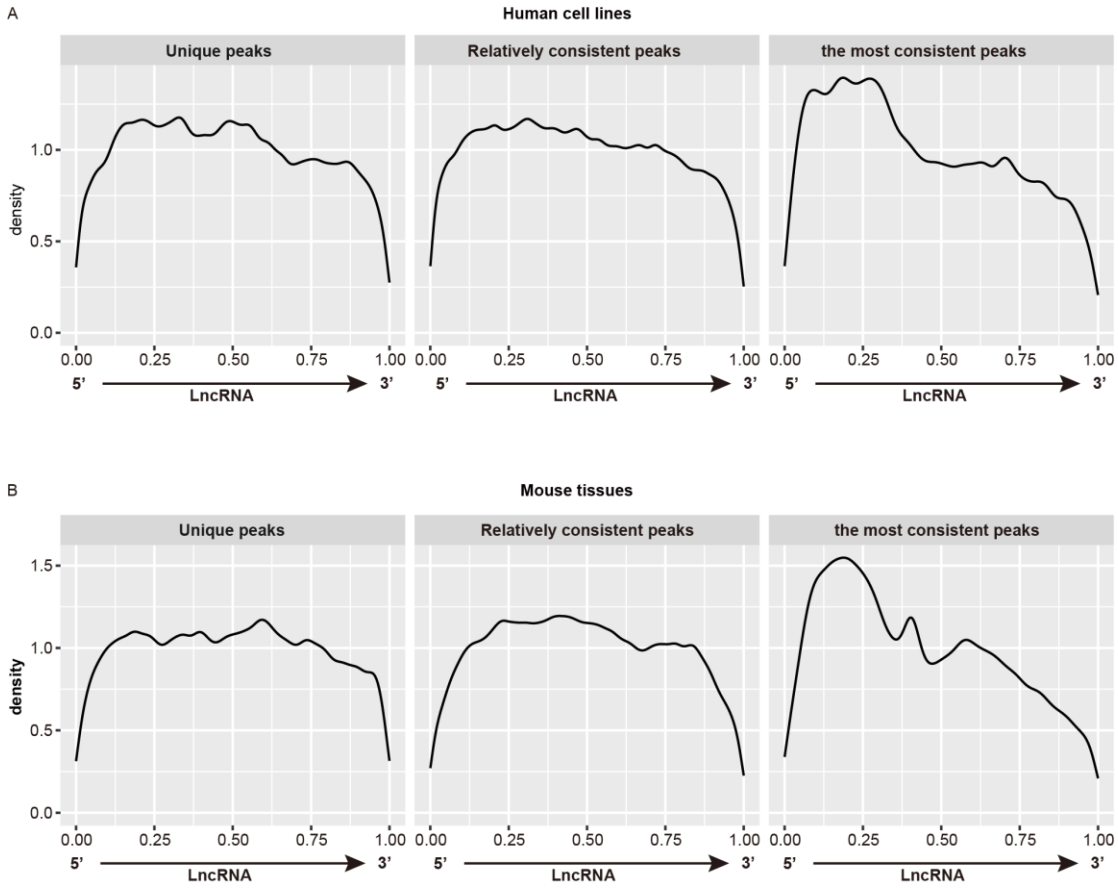

Supplementary Figure 10 The distribution patterns of m6A on lncRNA. The distribution of m6A sites with varying consistency levels on lncRNA across 8 human cell lines (A) and 11 mouse tissues (B).

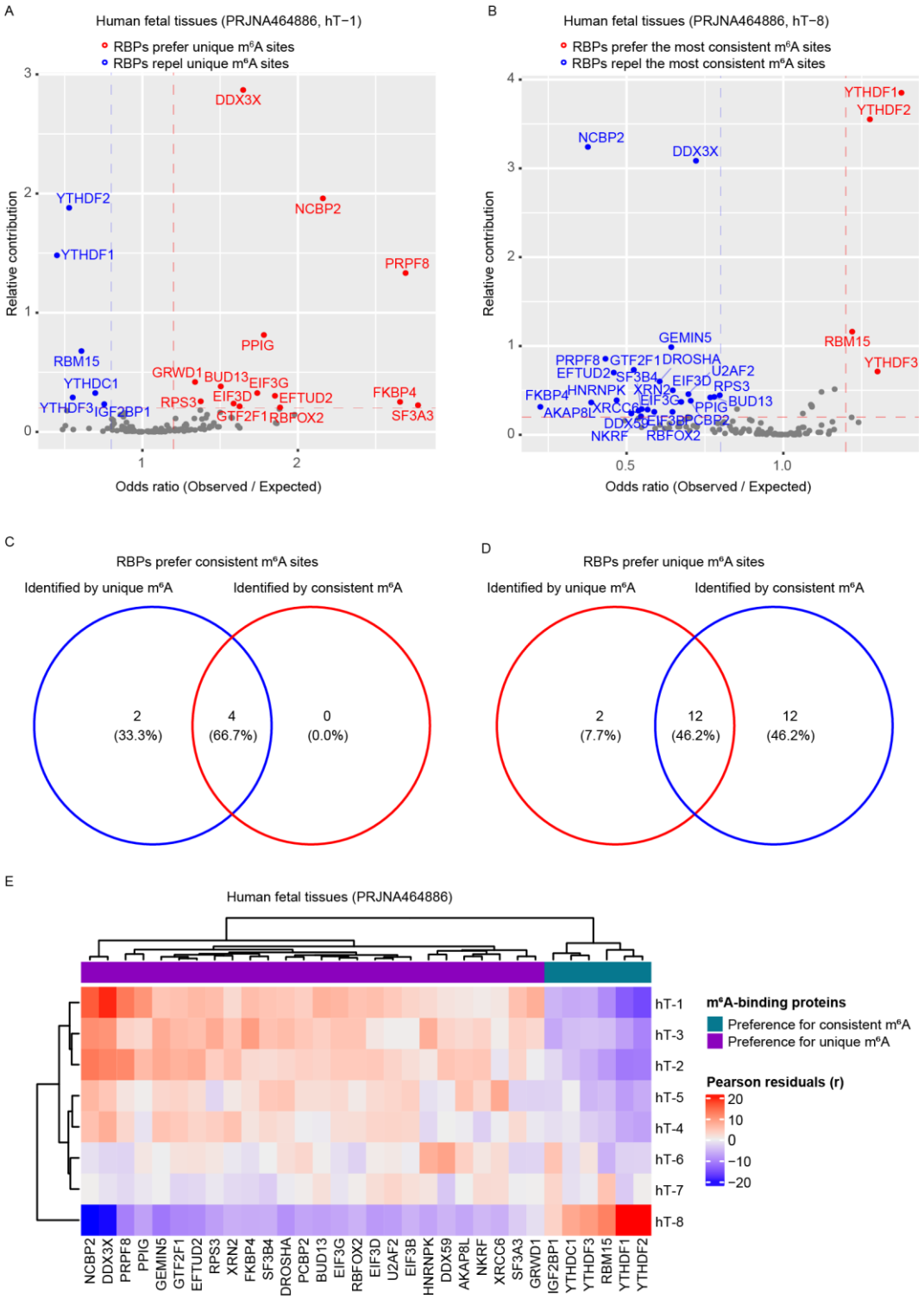

Supplementary Figure 11 **m6A-binding proteins identified by m6A sites of eight consistency levels in eight human fetal tissues.** A, Fourteen m6A-binding RBPs (red dots) that prefer binding to unique m6A sites and six m6A-binding RBPs (blue dots) that repel these sites are identified through unique m6A sites enrichment analysis. B, Four m6A-binding RBPs (red dots) that prefer binding to the most consistent m6A sites and twenty-four m6A-binding RBPs (blue dots) that repel these sites are identified through the most consistent m6A sites enrichment analysis. C, Overlap analysis of m6A-binding proteins that prefer binding to consistent m6A sites. D, Overlap analysis of m6A-binding

proteins that prefer binding to unique m6A sites. E, The affinity of thirty-two m6A-binding proteins to m6A sites of eight consistency levels in eight human fetal tissues. The thresholds: (1) Odds ratio >= 1.2 or Odds ratio <= 0.8; (2) relative contribution > 0.2 were used to identify RBPs with preference for m6A sites. Pearson residuals was used for showing preferential binding or avoidance.

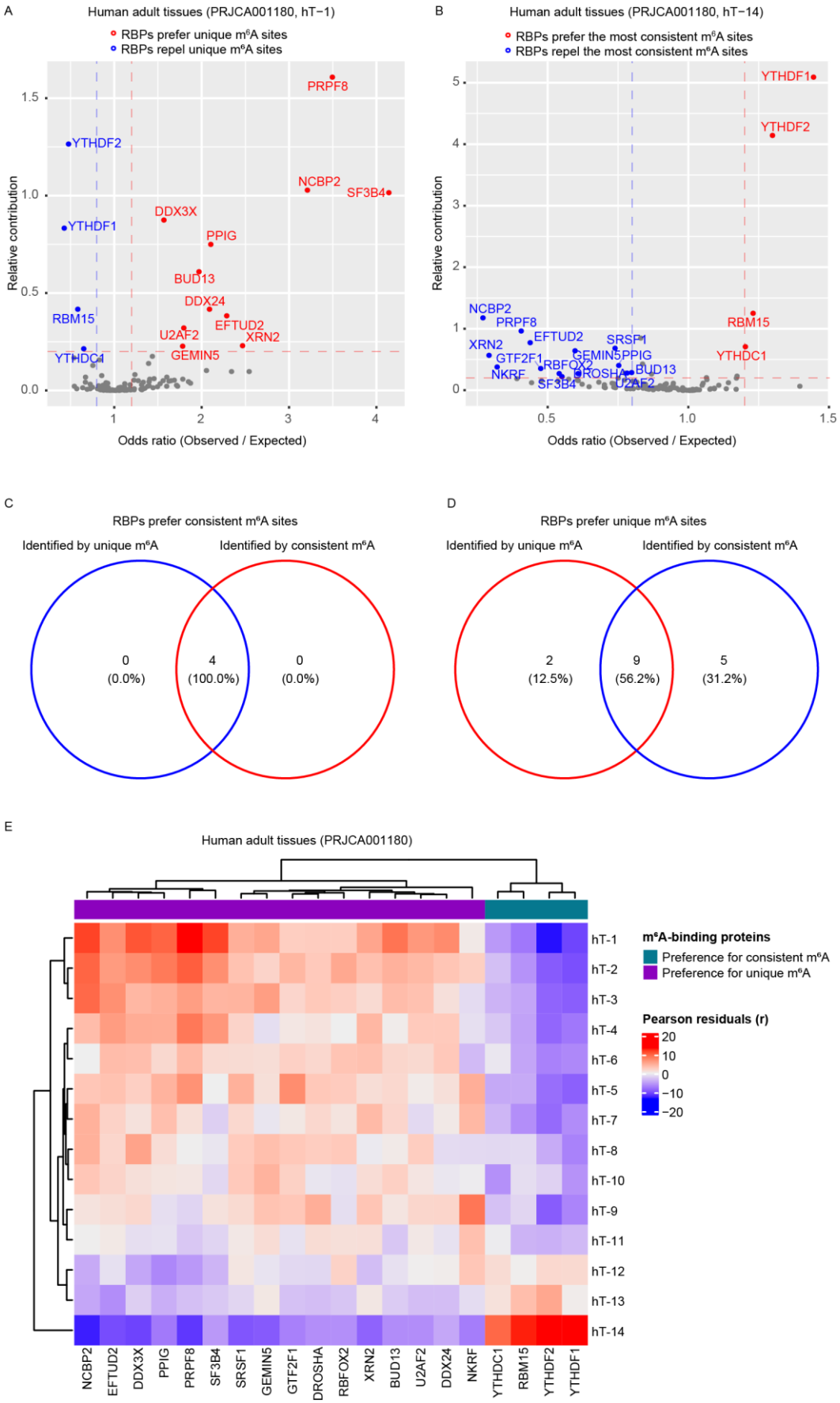

Supplementary Figure 12 **m6A-binding proteins identified by m6A sites of fourteen**

consistency levels in fourteen adult tissues. A, Eleven m6A-binding RBPs (red dots) that prefer binding to unique m6A sites and four m6A-binding RBPs (blue dots) that repel these sites are identified through unique m6A sites enrichment analysis. B, Four m6A-binding RBPs (red dots) that prefer binding to the most consistent m6A sites and fourteen m6A-binding RBPs (blue dots) that repel these sites are identified through the most consistent m6A sites enrichment analysis. C, Overlap analysis of m6A-binding proteins that prefer binding to consistent m6A sites. D, Overlap analysis of m6A-binding proteins that prefer binding to unique m6A sites. E, The affinity of twenty m6A-binding proteins to m6A sites of fourteen consistency levels in fourteen adult tissues. The thresholds: (1) Odds ratio >= 1.2 or Odds ratio <= 0.8; (2) relative contribution > 0.2 were used to identify RBPs with preference for m6A sites. Pearson residuals was used for showing preferential binding or avoidance.

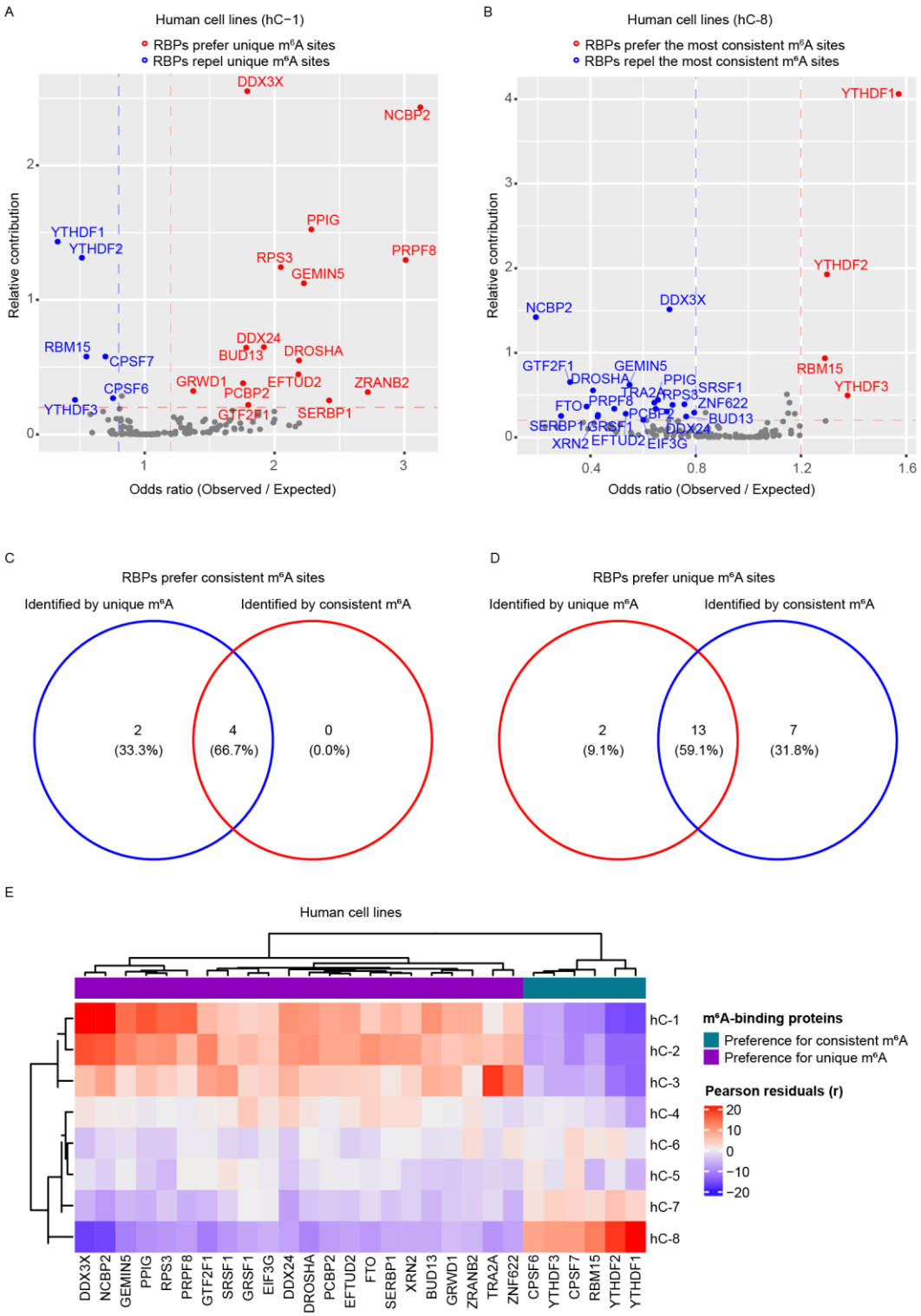

Supplementary Figure 13 **m6A-binding proteins identified by m6A sites of eight consistency levels in eight human cell lines.** A, Fifteen m6A-binding RBPs (red dots) that prefer binding to unique m6A sites and six m6A-binding RBPs (blue dots) that repel these sites are identified through unique m6A sites enrichment analysis. B, Four m6A-binding RBPs (red dots) that prefer binding to the most consistent m6A sites and twenty m6A-binding RBPs (blue dots) that repel these sites are identified through the most consistent m6A sites enrichment analysis. C, Overlap analysis of m6A-binding proteins that

prefer binding to consistent m6A sites. D, Overlap analysis of m6A-binding proteins that prefer binding to unique m6A sites. E, The affinity of twenty-eight m6A-binding proteins to m6A sites of eight consistency levels in eight human cell lines. The thresholds: (1) Odds ratio >= 1.2 or Odds ratio <= 0.8; (2) relative contribution > 0.2 were used to identify RBPs with preference for m6A sites. Pearson residuals was used for showing preferential binding or avoidance.

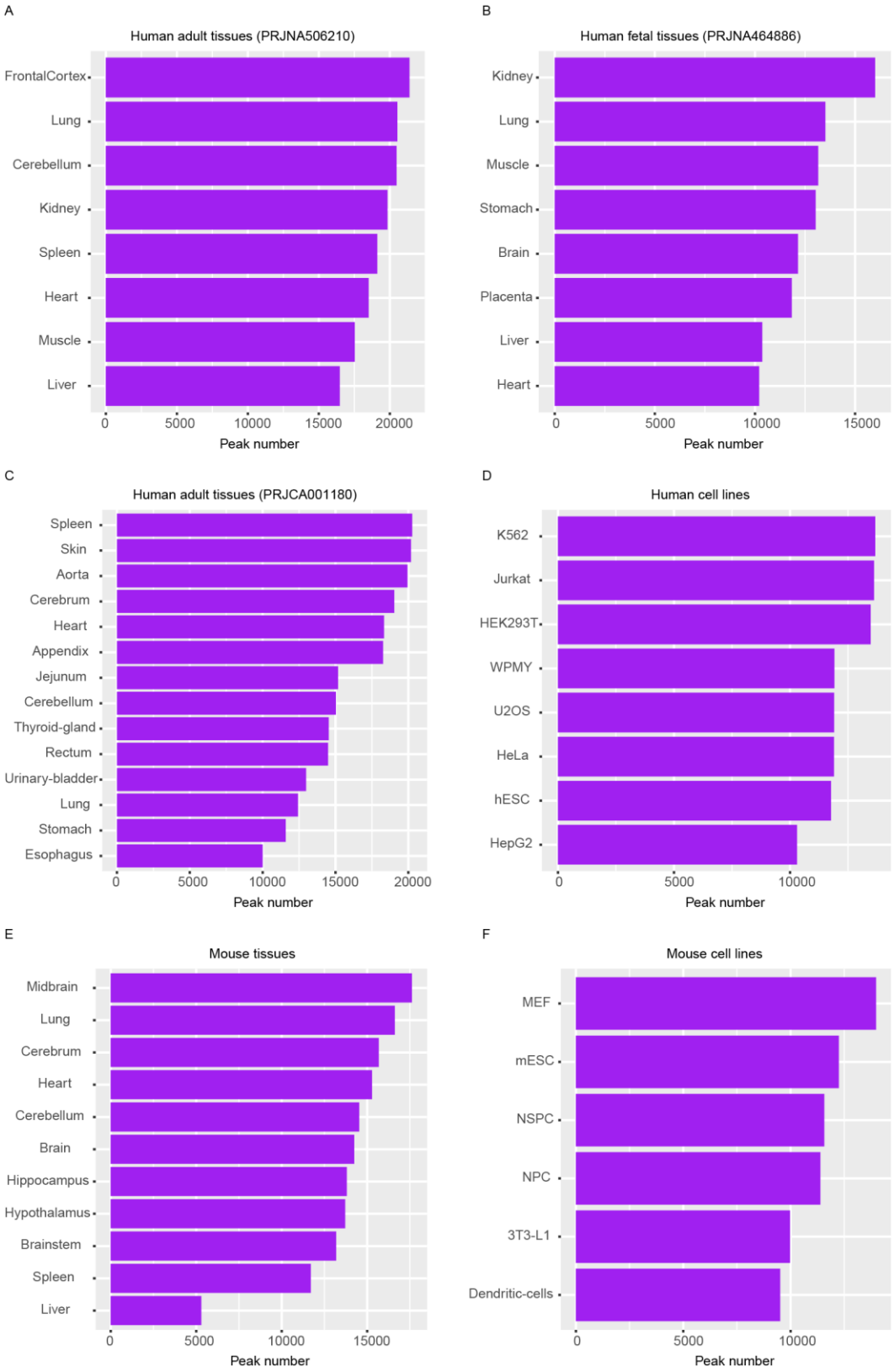

Supplementary Figure 14 **Number of mRNA-consistent m6A sites in different tissues and cell lines.** A-F, Number of mRNA-consistent m6A sites in eight adult tissues (A), eight human fetal tissues (B), fourteen adult tissues (C), eight human cell lines (D), eleven mouse tissues (E), and six mouse cell lines (F).

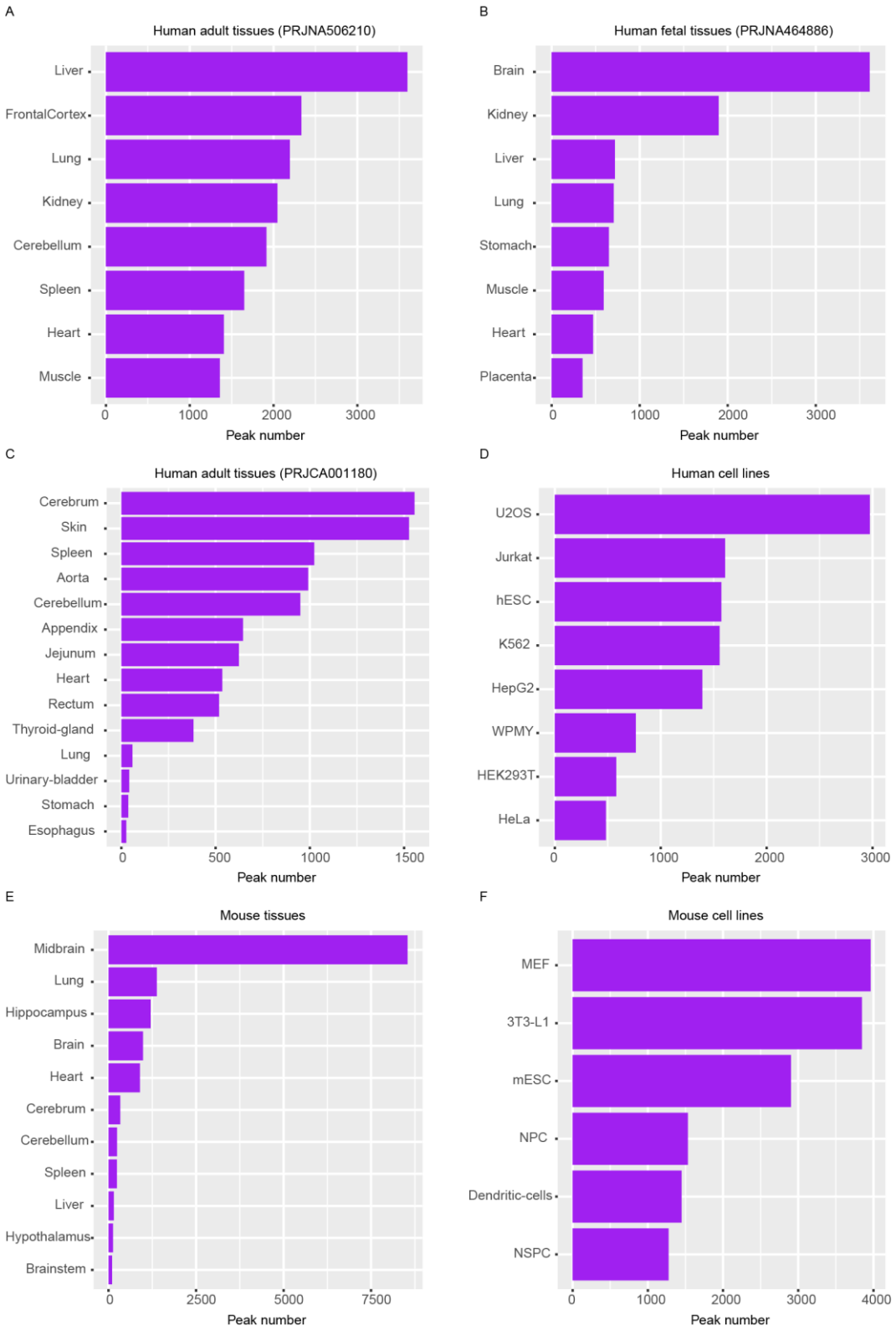

Supplementary Figure 15 **Number of mRNA-unique m6A sites in different tissues and cell lines.** A-F, Number of mRNA-unique m6A sites in eight adult tissues (A), eight human fetal tissues (B), fourteen adult tissues (C), eight human cell lines (D), eleven mouse tissues (E), and six mouse cell lines (F).

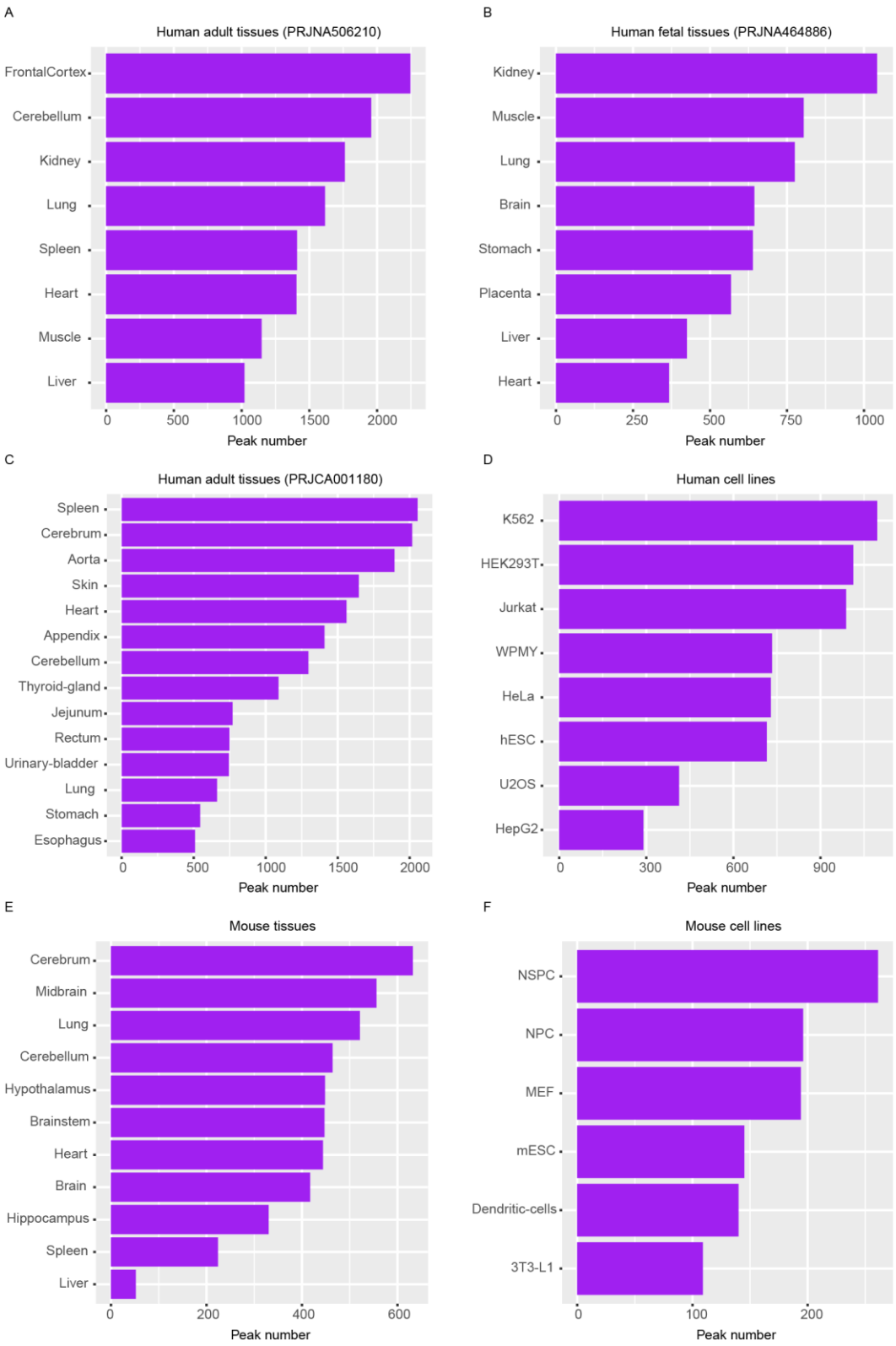

Supplementary Figure 16 **Number of lncRNA-consistent m6A sites in different tissues and cell lines.** A-F, Number of lncRNA-consistent m6A sites in eight adult tissues (A), eight human fetal tissues (B), fourteen adult tissues (C), eight human cell lines (D), eleven mouse tissues (E), and six mouse cell lines (F).

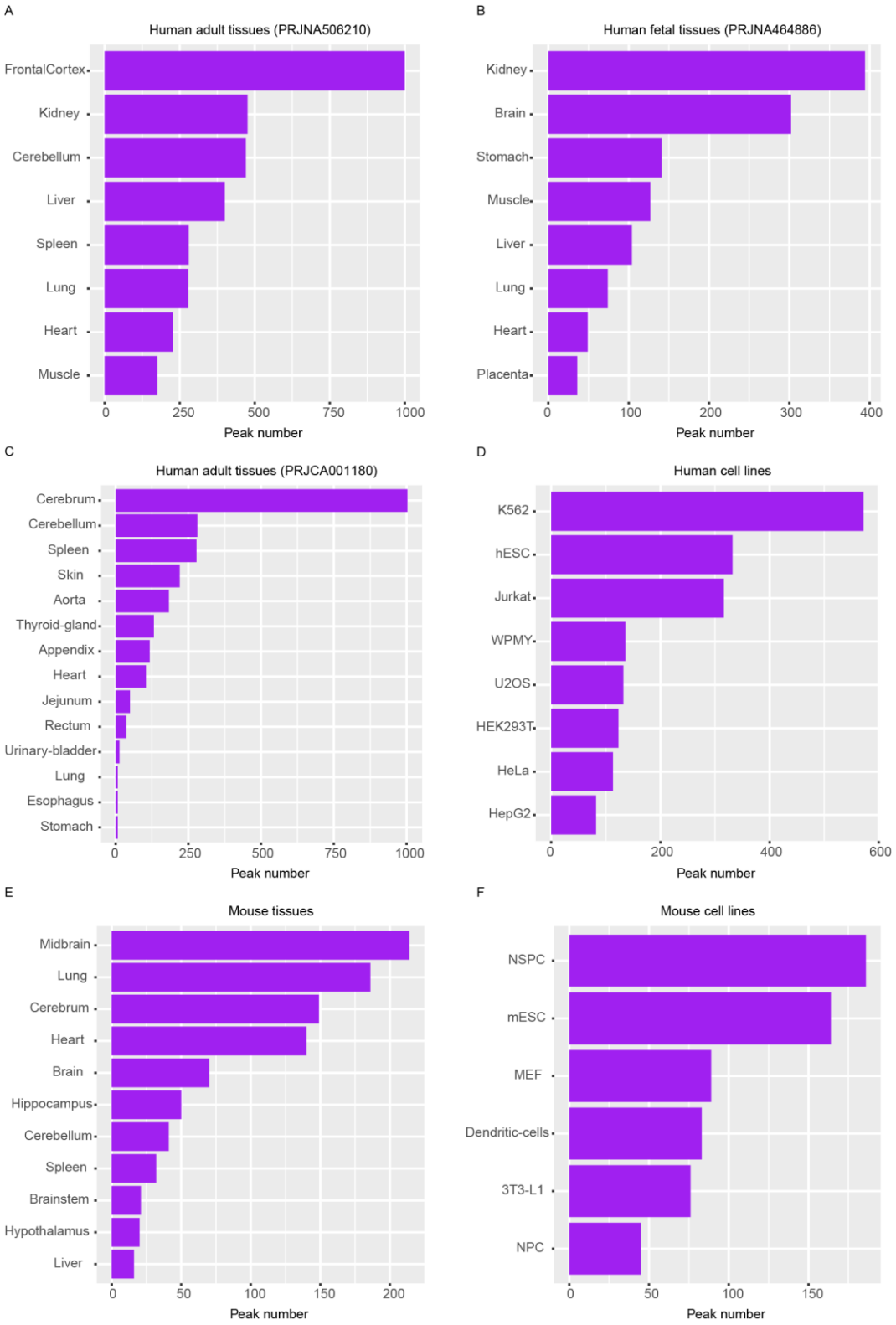

Supplementary Figure 17 **Number of lncRNA-unique m6A sites in different tissues and cell lines.** A-F, Number of lncRNA-unique m6A sites in eight adult tissues (A), eight human fetal tissues (B), fourteen adult tissues (C), eight human cell lines (D), eleven mouse tissues (E), and six mouse cell lines (F).

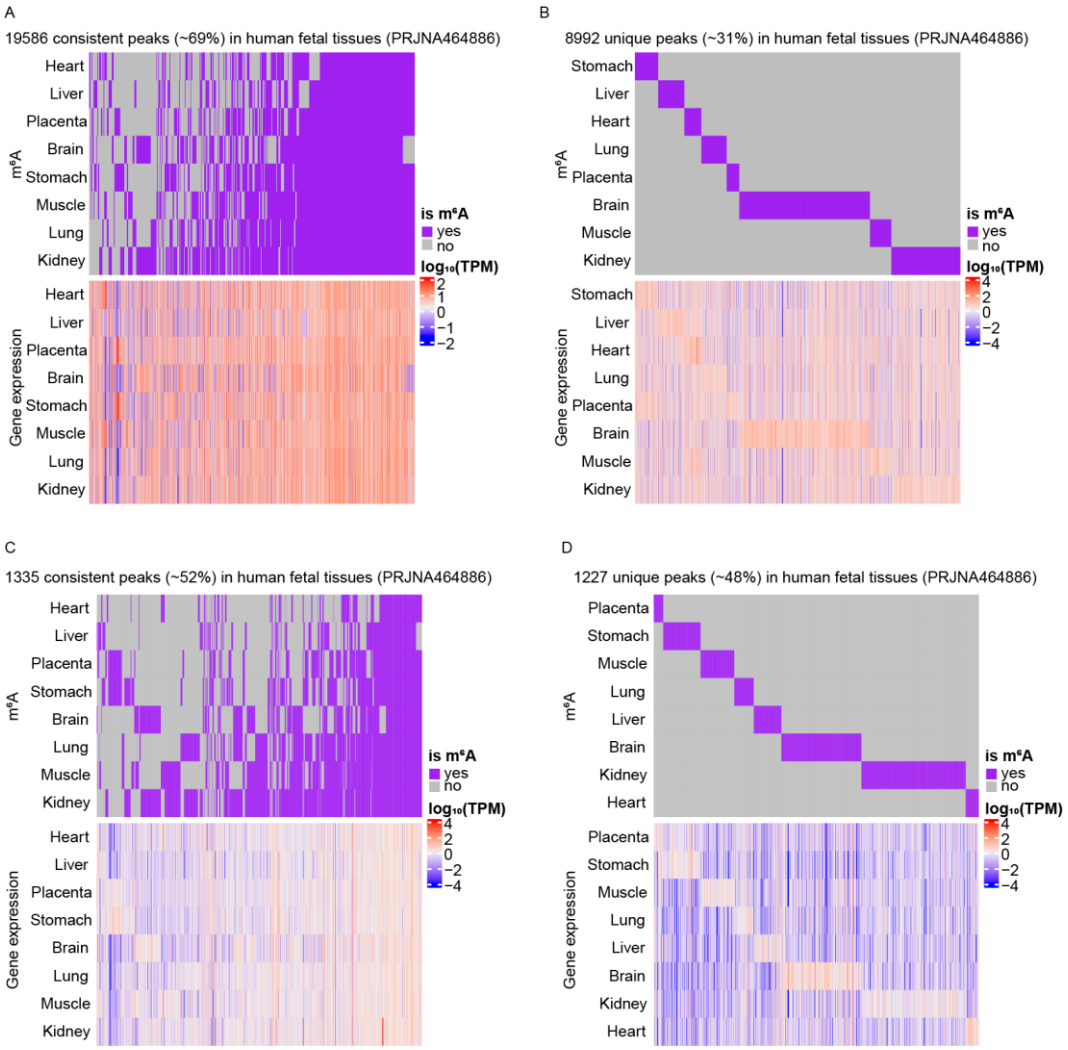

Supplementary Figure 18 **mRNA and lncRNA m6A modification and gene expression profiles in eight different human fetal tissues.** A, mRNA-consistent m6A sites and expression levels of genes marked by these sites. B, mRNA-unique m6A sites and expression levels of genes marked by these sites. C, lncRNA-consistent m6A sites and expression levels of genes marked by these sites. D, lncRNA-unique m6A sites and expression levels of genes marked by these sites. Rows denote different tissues, and columns denote different m6A sites (upper panel) and genes marked by these sites (lower panel).

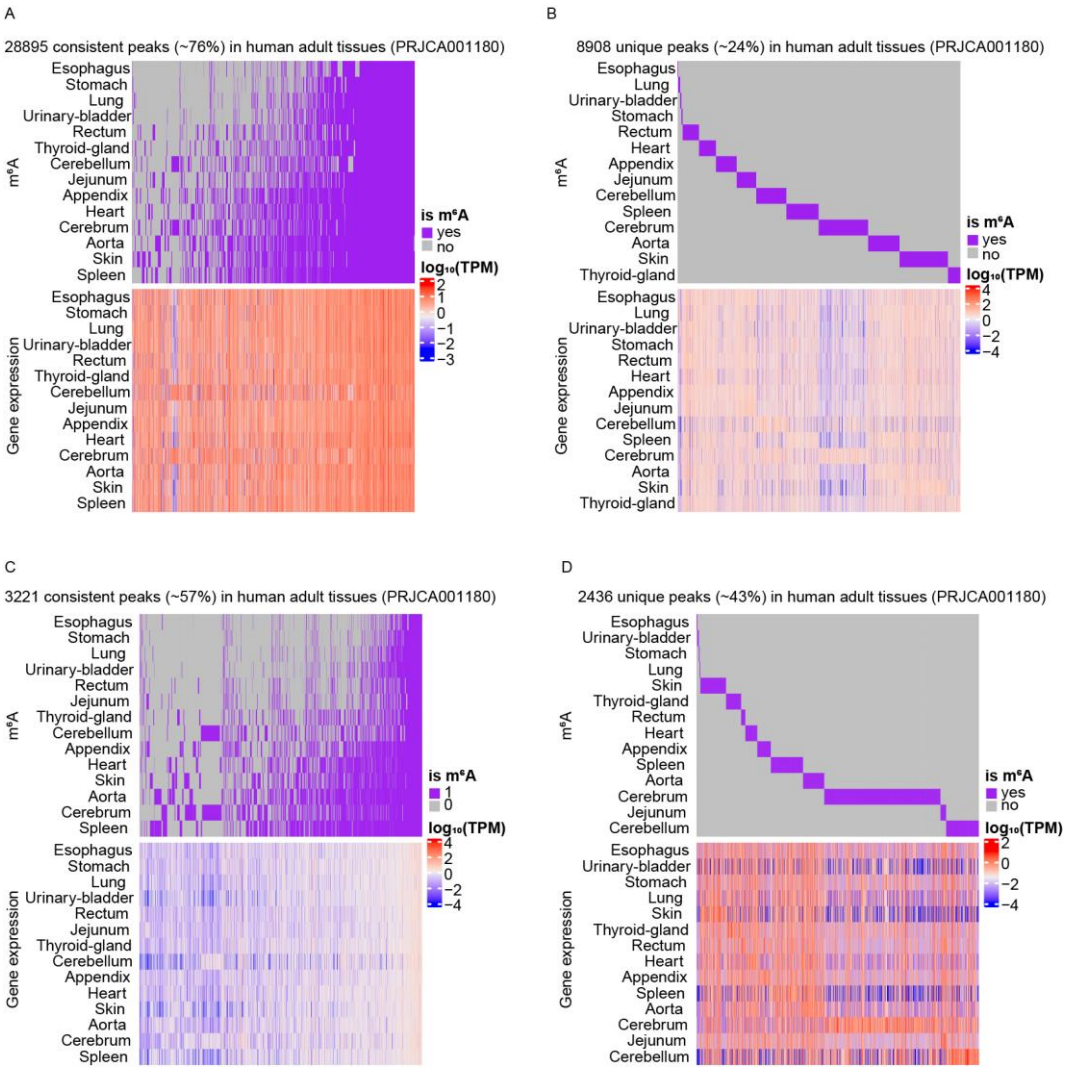

Supplementary Figure 19 **mRNA and lncRNA m6A modification and gene expression profiles in fourteen different adult tissues.** A, mRNA-consistent m6A sites and expression levels of genes marked by these sites. B, mRNA-unique m6A sites and expression levels of genes marked by these sites. C, lncRNA-consistent m6A sites and expression levels of genes marked by these sites. D, lncRNA-unique m6A sites and expression levels of genes marked by these sites. Rows denote different tissues, and columns denote different m6A sites (upper panel) and genes marked by these sites (lower panel).

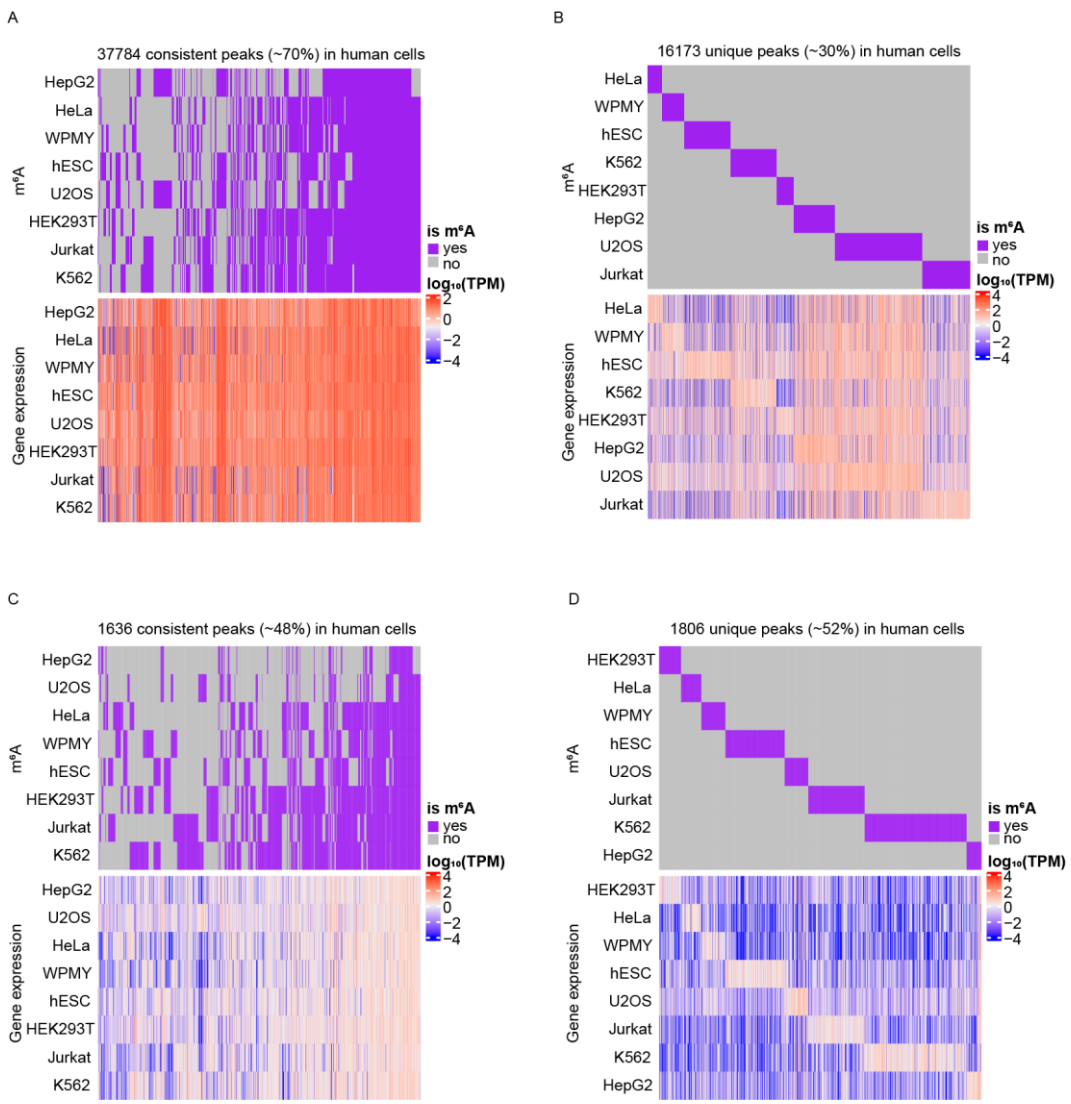

Supplementary Figure 20 **mRNA and lncRNA m6A modification and gene expression profiles in eight different human cell lines.** A, mRNA-consistent m6A sites and expression levels of genes marked by these sites. B, mRNA-unique m6A sites and expression levels of genes marked by these sites. C, lncRNA-consistent m6A sites and expression levels of genes marked by these sites. D, lncRNA-unique m6A sites and expression levels of genes marked by these sites. Rows denote different tissues, and columns denote different m6A sites (upper panel) and genes marked by these sites (lower panel).

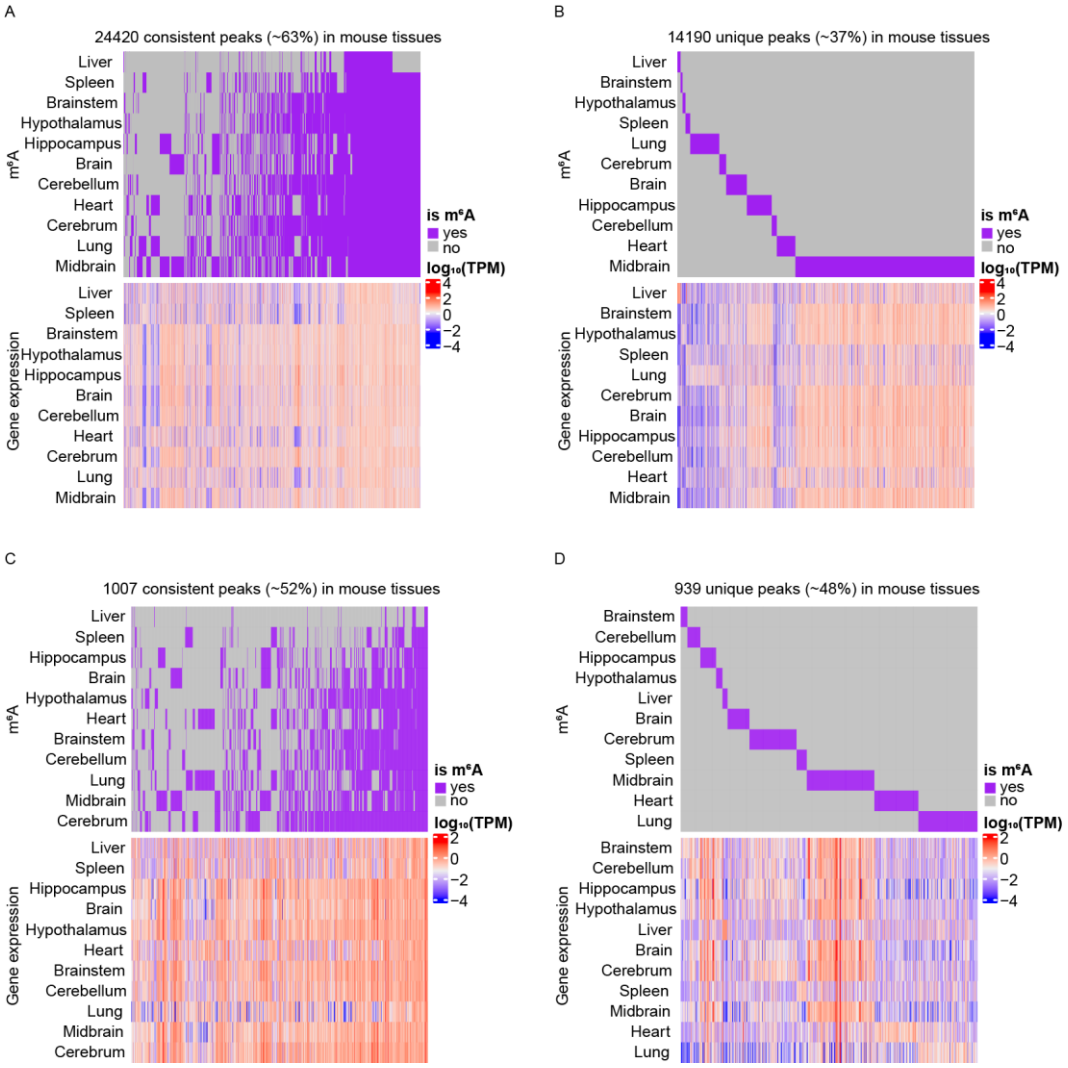

Supplementary Figure 21 **mRNA and lncRNA m6A modification and gene expression profiles in eleven different mouse tissues.** A, mRNA-consistent m6A sites and expression levels of genes marked by these sites. B, mRNA-unique m6A sites and expression levels of genes marked by these sites. C, lncRNA-consistent m6A sites and expression levels of genes marked by these sites. D, lncRNA-unique m6A sites and expression levels of genes marked by these sites. Rows denote different tissues, and columns denote different m6A sites (upper panel) and genes marked by these sites (lower panel).

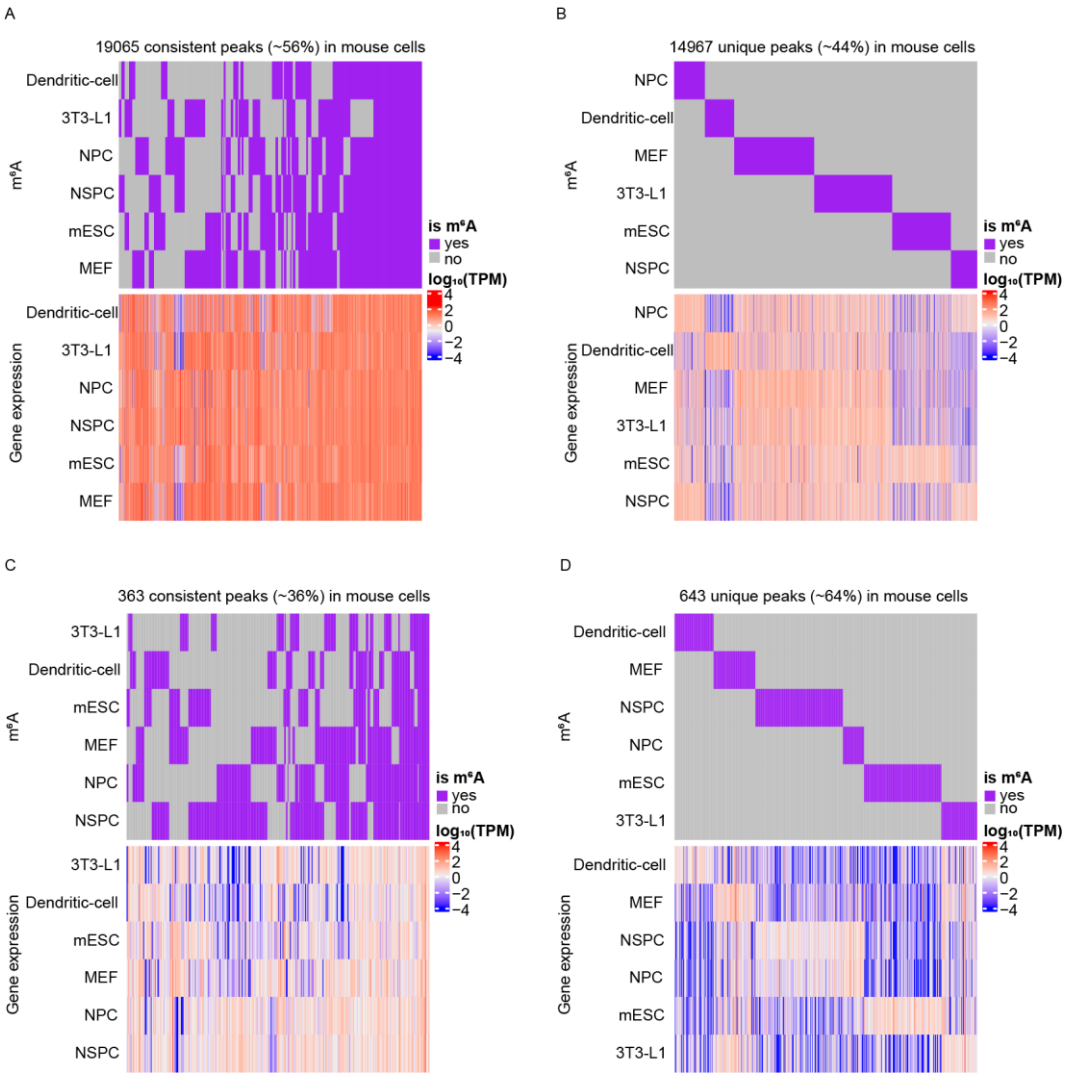

Supplementary Figure 22 **mRNA and lncRNA m6A modification and gene expression profiles in six different mouse cell lines.** A, mRNA-consistent m6A sites and expression levels of genes marked by these sites. B, mRNA-unique m6A sites and expression levels of genes marked by these sites. C, lncRNA-consistent m6A sites and expression levels of genes marked by these sites. D, lncRNA-unique m6A sites and expression levels of genes marked by these sites. Rows denote different tissues, and columns denote different m6A sites (upper panel) and genes marked by these sites (lower panel).

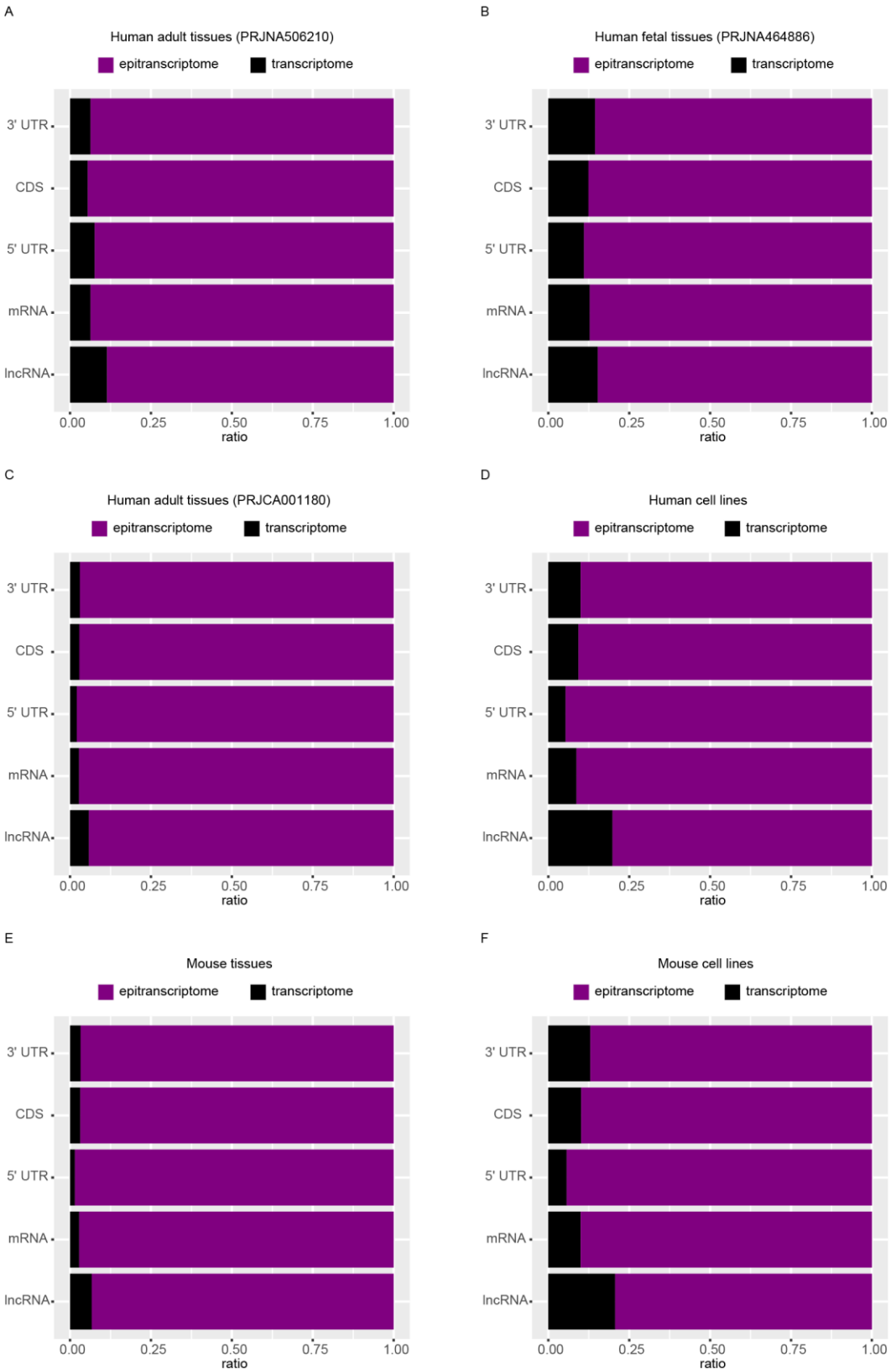

Supplementary Figure 23 **The proportion of transcriptome-specific and epi-transcriptome-specific m6A sites in mRNA, lncRNA, mRNA 5'-UTR, CDS, and 3'-UTR.** A-F, The proportion of transcriptome-specific m6A sites and epi-transcriptomes-specific m6A sites in eight adult tissues (A), eight human fetal tissues (B), fourteen adult tissues

(C), eight human cell lines (D), eleven mouse tissues (E), and six mouse cell lines (F).

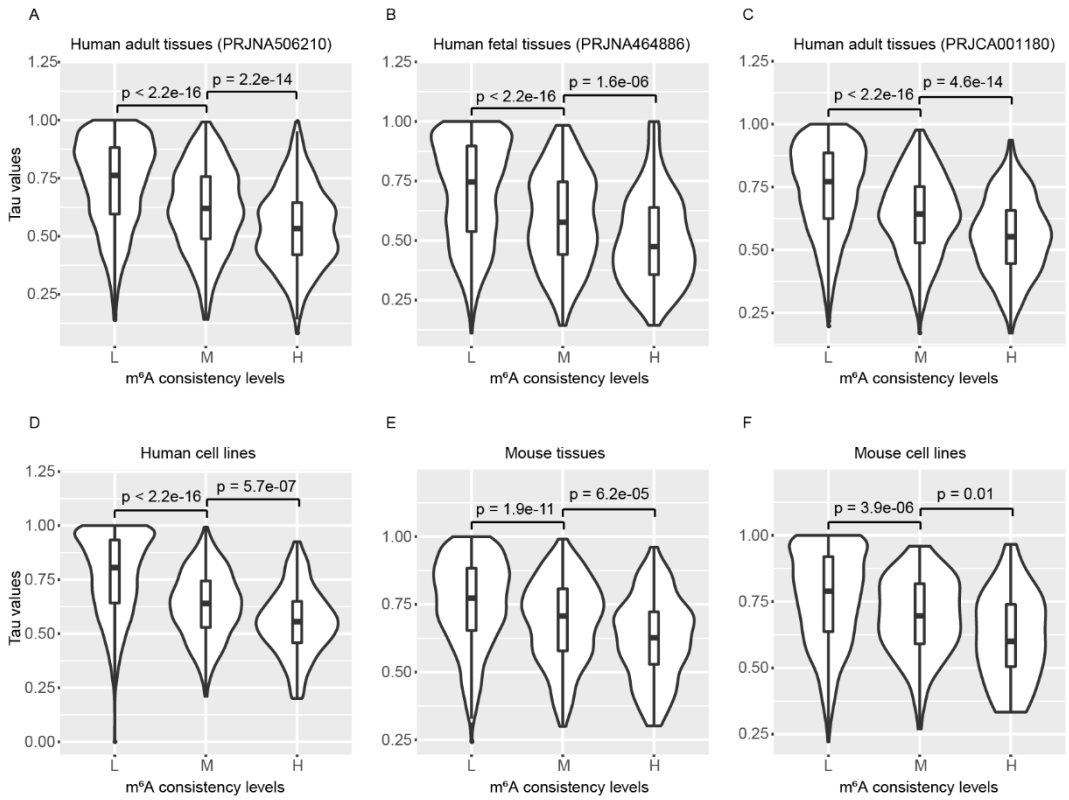

Supplementary Figure 24 **lncRNA m6A site consistency levels positively correlated with gene expression homeostasis.** A, Relative expression stability of m6A-modified genes (L, M, and H sets containing 3037, 706, and 468 lncRNA genes, respectively) among eight different adult tissues. B, Relative expression stability of m6A-modified genes (L, M, and H sets containing 1378, 345, and 184 lncRNA genes, respectively) among eight different human fetal tissues. C, Relative expression stability of m6A-modified genes (L, M, and H sets containing 2740, 604, and 327 lncRNA genes, respectively) among fourteen different adult tissues. D, Relative expression stability of m6A-modified genes (L, M, and H sets containing 1788, 434, and 140 lncRNA genes, respectively) among eight different human cell lines. E, Relative expression stability of m6A-modified genes (L, M, and H sets containing 1074, 290, and 152 lncRNA genes, respectively) among eleven different mouse tissues. F, Relative expression stability of m6A-modified genes (L, M, and H sets containing 618, 120, and 33 lncRNA genes, respectively) among six different mouse cell lines. Significance was evaluated by the two-sided Mann-Whitney test.

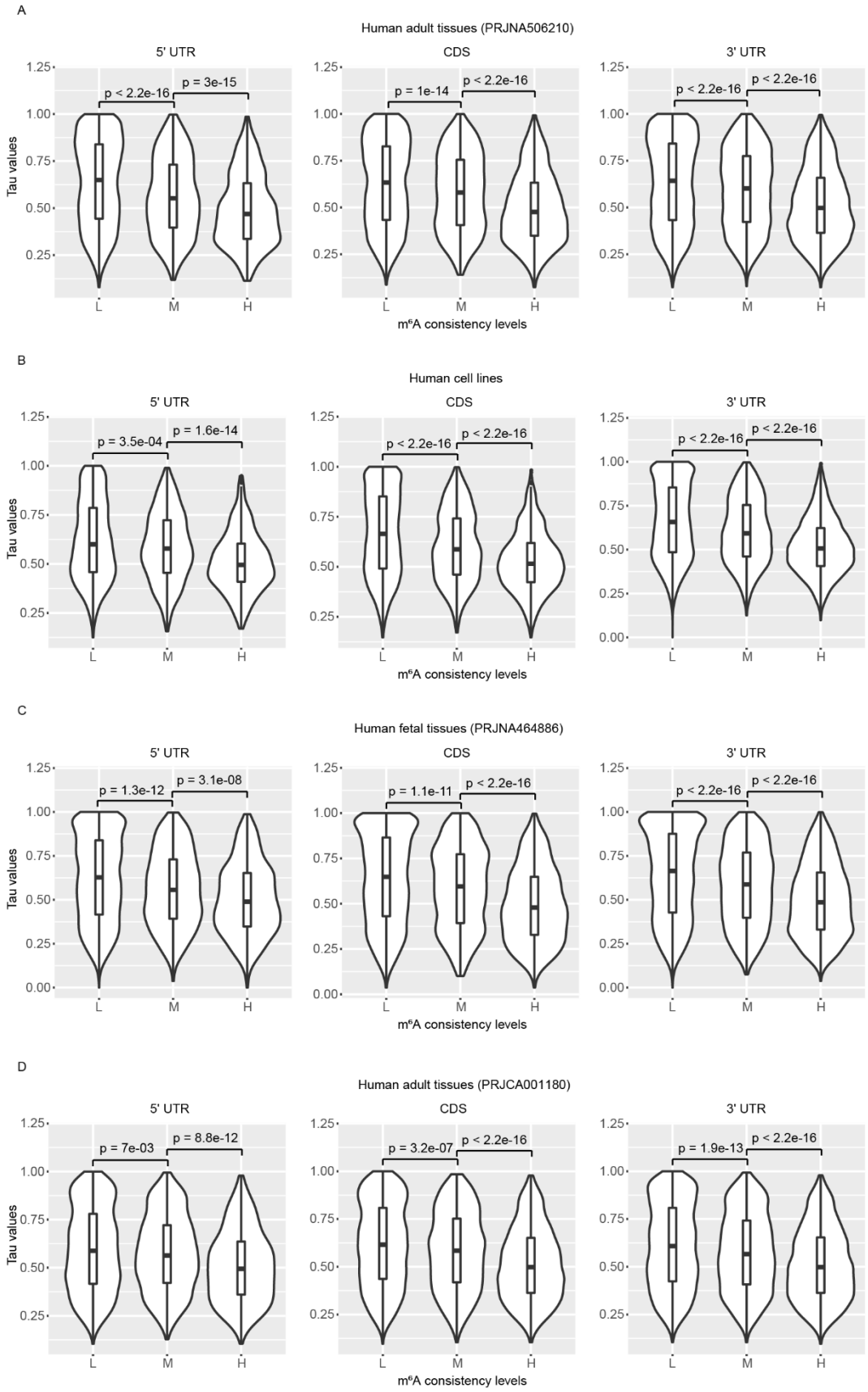

Supplementary Figure 25 **Consistency levels of m6A sites in the mRNA 5'-UTR, CDS, and 3'-UTR positively correlated with gene expression homeostasis.** A, Relative expression stability of m6A-modified genes (for 5'-UTR, L, M, and H sets containing 5124,

1257, and 969 mRNA genes, respectively; for CDS, L, M, and H sets containing 5561, 1746, and 1925 mRNA genes, respectively; for 3'-UTR, L, M, and H sets containing 8060, 3894, and 5916 mRNA genes, respectively) among eight different adult tissues. B, Relative expression stability of m6A-modified genes (for 5'-UTR, L, M, and H sets containing 3699, 780, and 483 mRNA genes, respectively; for CDS, L, M, and H sets containing 4199, 1536, and 1235 mRNA genes, respectively; for 3'-UTR, L, M, and H sets containing 6276, 3253, and 3468 mRNA genes, respectively) among eight different human cell lines. C, Relative expression stability of m6A-modified genes (for 5'-UTR, L, M, and H sets containing 3522, 1005, and 854 mRNA genes, respectively; for CDS, L, M, and H sets containing 3562, 1398, and 1783 mRNA genes, respectively; for 3'-UTR, L, M, and H sets containing 4744, 2465, and 3742 mRNA genes, respectively) among eight different human fetal tissues. D, Relative expression stability of m6A-modified genes (for 5'-UTR, L, M, and H sets containing 3219, 1017, and 841 mRNA genes, respectively; for CDS, L, M, and H sets containing 4615, 1603, and 2143 mRNA genes, respectively; for 3'-UTR, L, M, and H sets containing 6916, 3275, and 5311 mRNA genes, respectively) among fourteen different adult tissues. Significance was evaluated by the two-sided Mann-Whitney test.

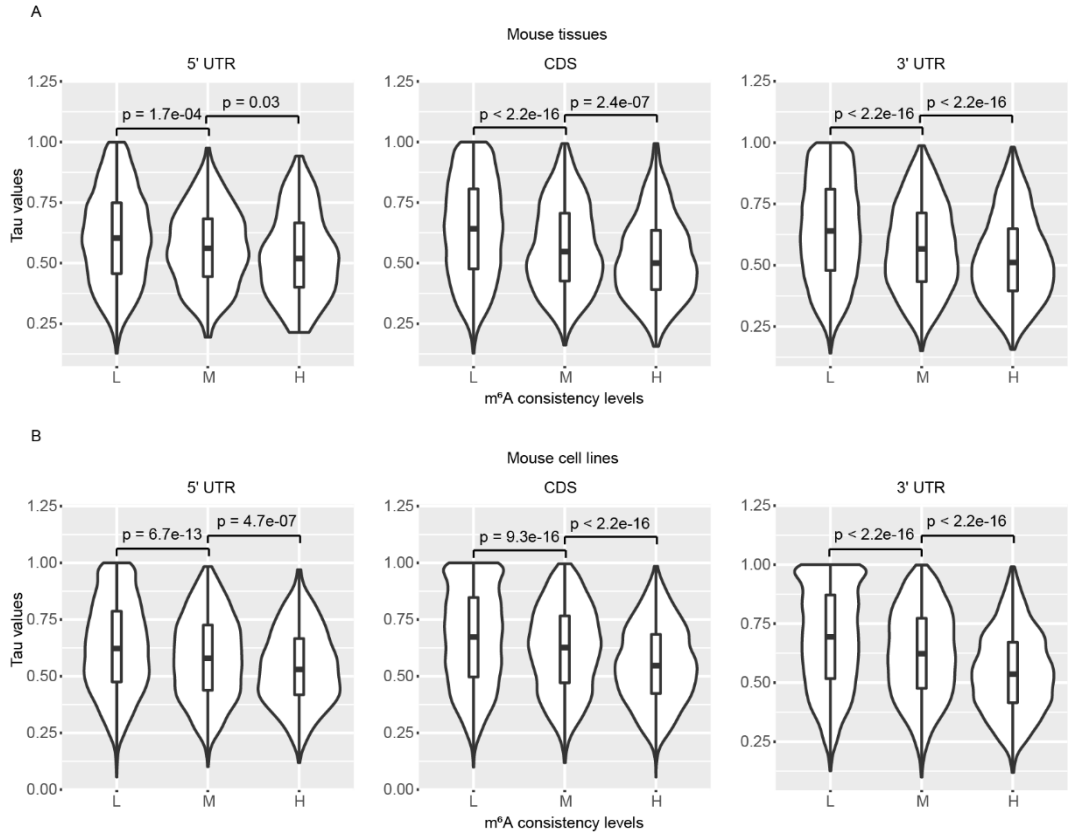

Supplementary Figure 26 **Consistency levels of m6A sites in the mRNA 5'-UTR, CDS, and 3'-UTR positively correlated with gene expression homeostasis.** A, Relative expression stability of m6A-modified genes (for 5'-UTR, L, M, and H sets containing 4844, 325, and 144 mRNA genes, respectively; for CDS, L, M, and H sets containing 5923, 1258, and 756 mRNA genes, respectively; for 3'-UTR, L, M, and H sets containing 9445, 2776, and 2273 mRNA genes, respectively) among eleven different mouse tissues. B, Relative expression stability of m6A-modified genes (for 5'-UTR, L, M, and H sets containing 5185, 1432, and 656 mRNA genes, respectively; for CDS, L, M, and H sets containing 4723, 1525, and 1376 mRNA genes, respectively; for 3'-UTR, L, M, and H sets containing 5902, 2801, and 3318 mRNA genes, respectively) among six different mouse cell lines. Significance was evaluated by the two-sided Mann-Whitney test.

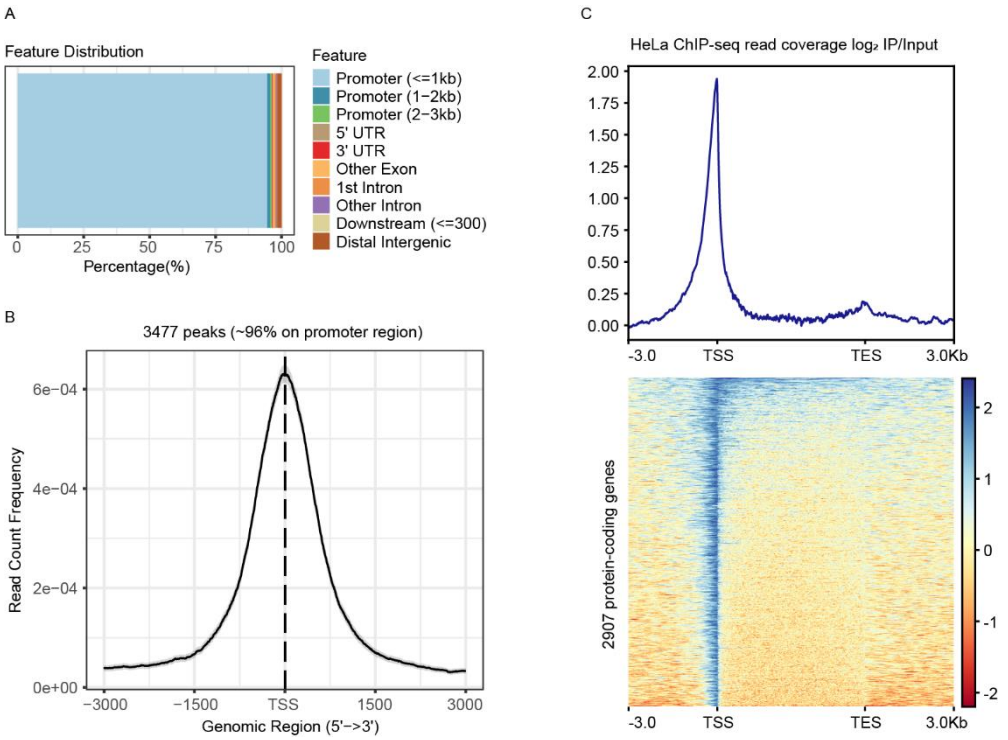

Supplementary Figure 27 **Distribution of METTL3 binding sites on the genome for HeLa.** A, Distribution of METTL3 binding sites in different genomic regions. B, The METTL3 binding sites were significantly enriched near the transcription start site (TSS). C, Distribution of METTL3 ChIP-seq read signal in 2907 protein-coding genes and their upstream and downstream 3Kb regions.

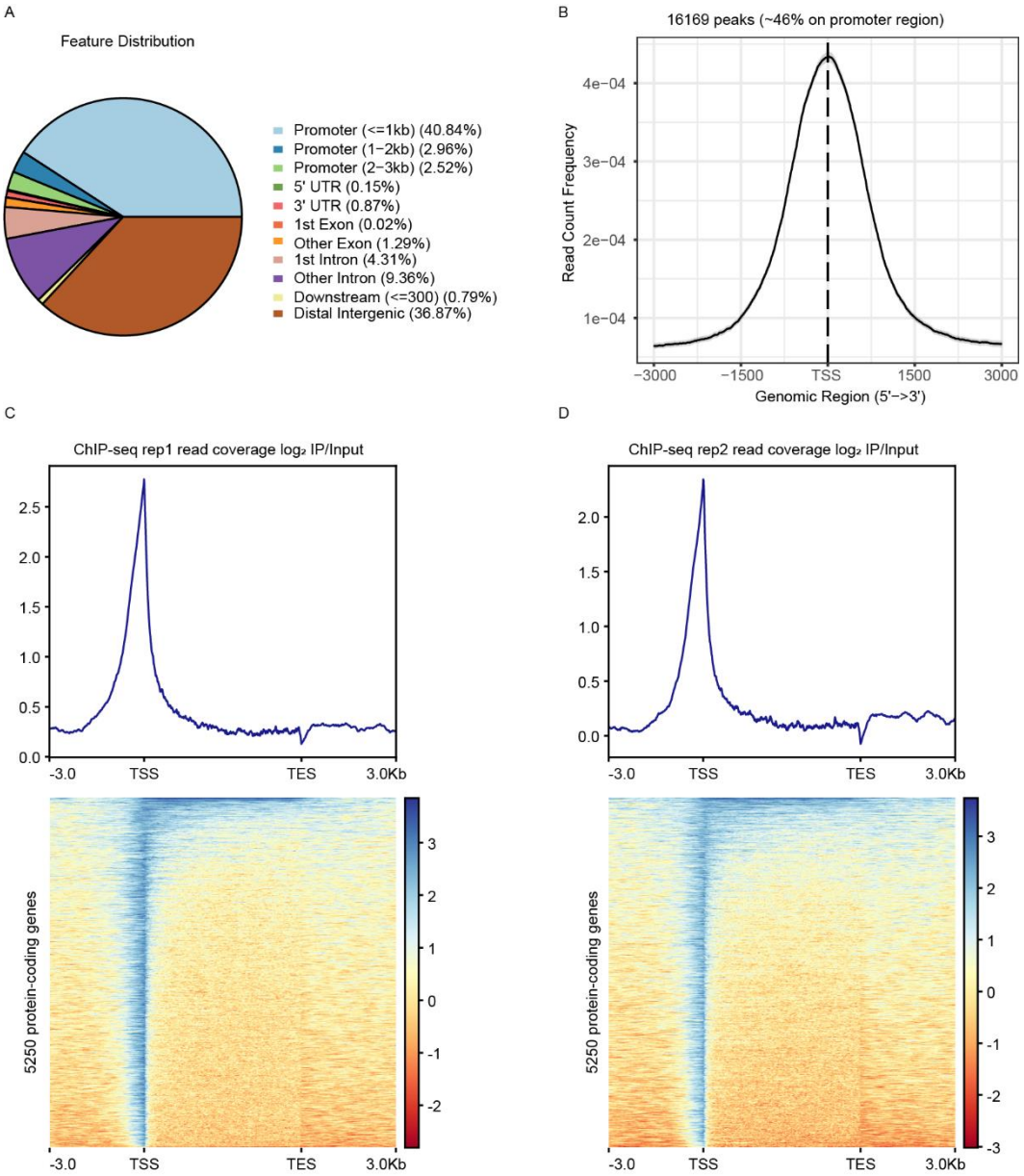

Supplementary Figure 28 **Distribution of METTL3 binding sites on the genome for mESC.** A, Distribution of METTL3 binding sites in different genomic regions. B, The METTL3 binding sites are significantly enriched near the transcription start site (TSS). C, D, Distribution of METTL3 ChIP-seq read signal in 5250 protein-coding genes and their upstream and downstream 3Kb regions.

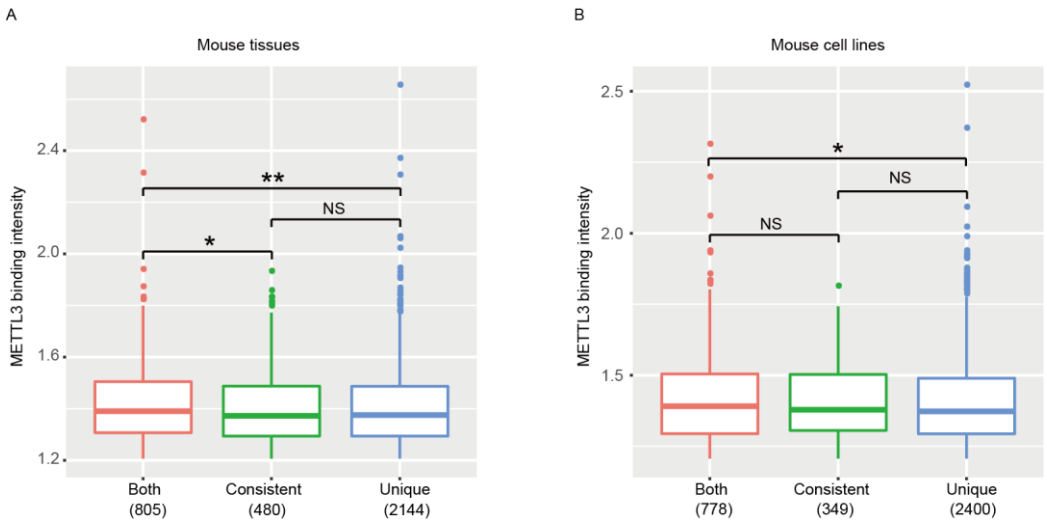

Supplementary Figure 29 **Binding intensity of METTL3 on three types of genes for mESC.** A, B, The METTL3-binding genes in mESC were classified into three categories, and METTL3 binding intensity was shown for mouse tissues (A) and mouse cell lines (B). Significance was evaluated by the two-sided Mann-Whitney test. An asterisk (*) denoted that the P value was between 0.01 and 0.05; Two asterisks (**) denoted that the P value was less than 0.01; Three asterisks (***) denoted that the P value was less than 0.001. NS denoted no significant difference. The numbers in parentheses denoted the number of genes.

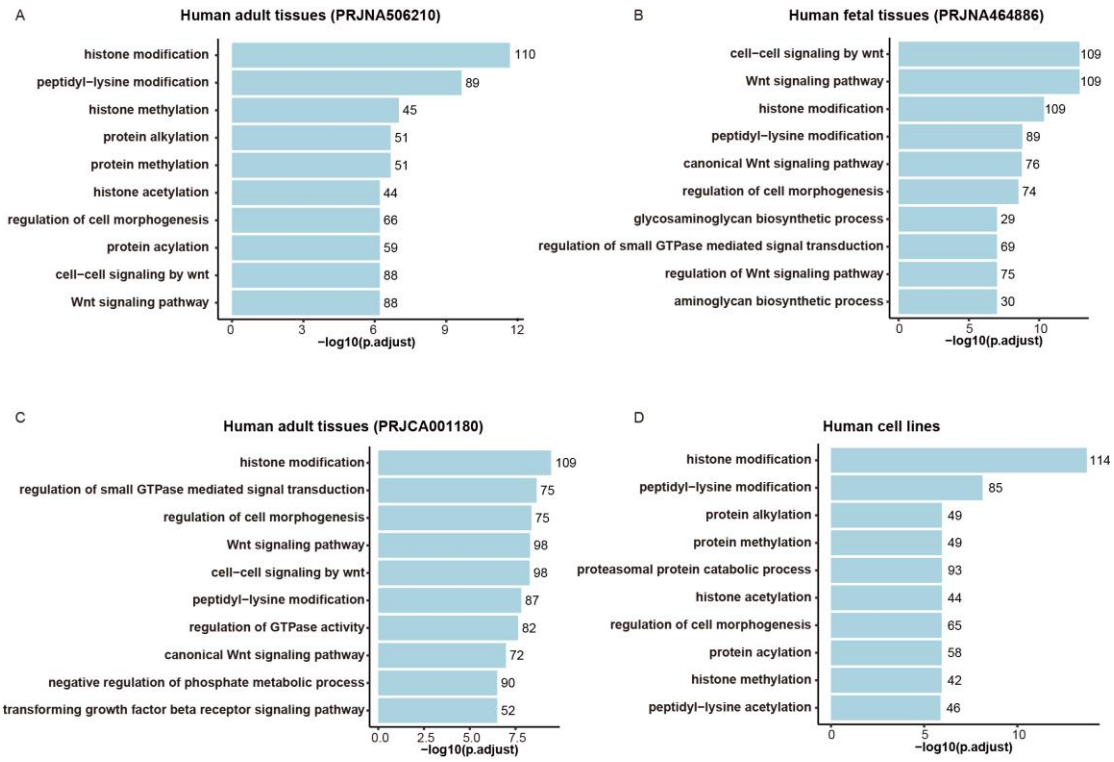

Supplementary Figure 30 The GO terms enriched for HeLa METTL3-binding protein-coding genes marked by the m6A sites with the highest consistency levels in 8 adult tissues (A), 8 fetal tissues (B), 14 adult tissues (C), and 8 human cell lines (D). Numbers represent the number of genes. Top 10 terms are shown.

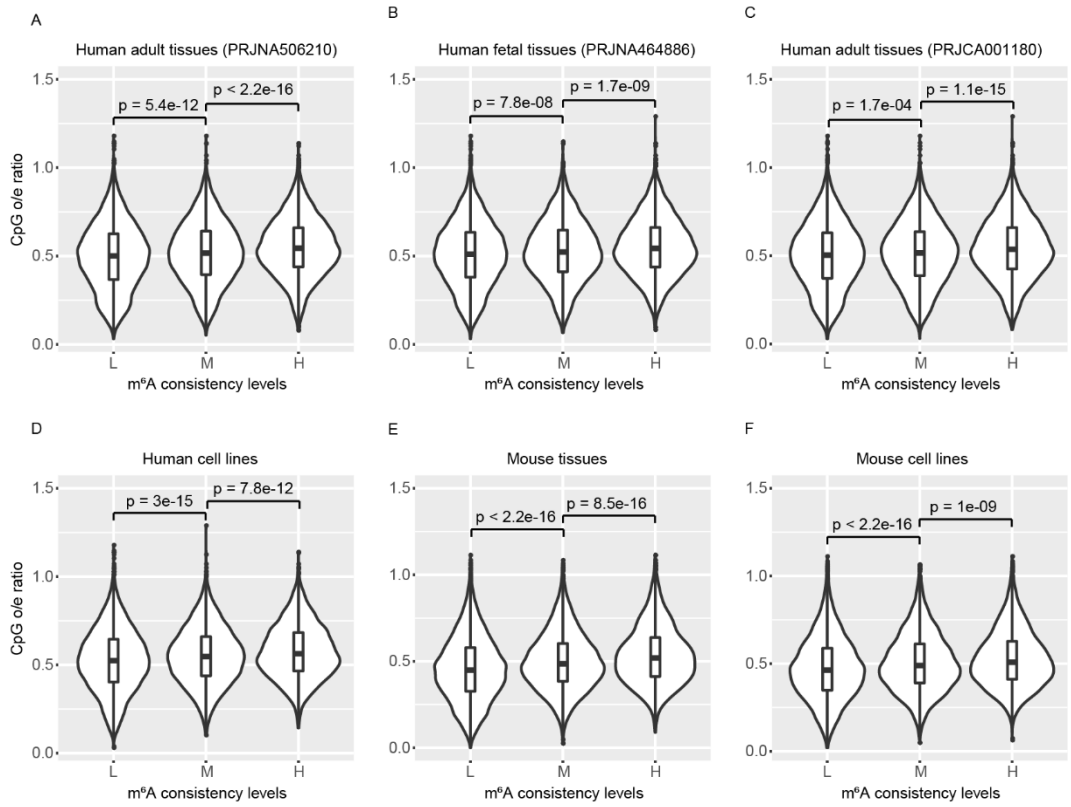

Supplementary Figure 31 **mRNA m6A consistency levels positively correlated with the CpG density of the gene promoter region**. A, CpG density of promoter regions of m6A-modified genes (L, M, and H sets containing 12228, 5824, and 7130 mRNA genes, respectively) among eight different adult tissues. B, CpG density of promoter regions of m6A-modified genes (L, M, and H sets containing 8735, 4242, and 5279 mRNA genes, respectively) among eight different human fetal tissues. C, CpG density of promoter regions of m6A-modified genes (L, M, and H sets containing 10470, 5104, and 6842 mRNA genes, respectively) among fourteen different adult tissues. D, CpG density of promoter regions of m6A-modified genes (L, M, and H sets containing 10031, 4769, and 4442 mRNA genes, respectively) among eight different human cell lines. E, CpG density of promoter regions of m6A-modified genes (L, M, and H sets containing 12906, 3913, and 2913 mRNA genes, respectively) among eleven different mouse tissues. F, CpG density of promoter regions of m6A-modified genes (L, M, and H sets containing 10653, 4754, and 4449 mRNA genes, respectively) among six different mouse cell lines. Significance was evaluated by the two-sided Mann-Whitney test.

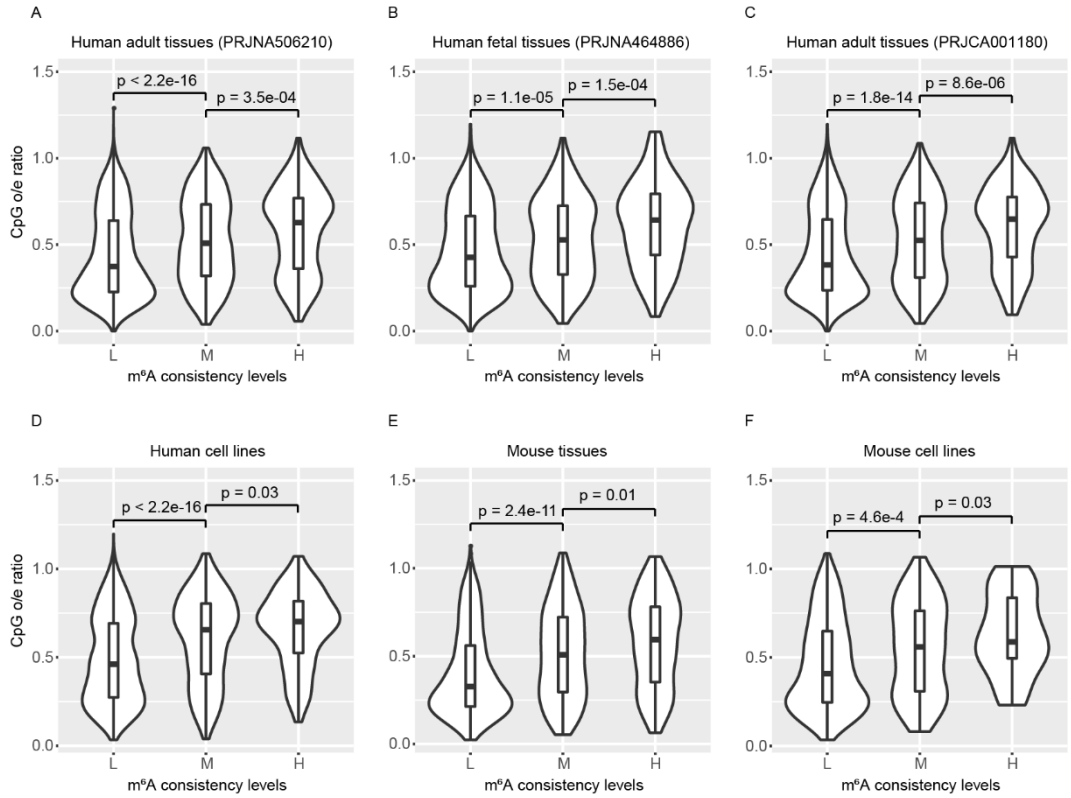

Supplementary Figure 32 **lncRNA m6A consistency levels positively correlated with the CpG density of the lncRNA gene promoter region.** A, CpG density of promoter regions of m6A-modified genes (L, M, and H sets containing 3037, 706, and 468 lncRNA genes, respectively) among eight different adult tissues. B, CpG density of promoter regions of m6A-modified genes (L, M, and H sets containing 1378, 345, and 184 lncRNA genes, respectively) among eight different human fetal tissues. C, CpG density of promoter regions of m6A-modified genes (L, M, and H sets containing 2740, 604, and 327 lncRNA genes, respectively) among fourteen different adult tissues. D, CpG density of promoter regions of m6A-modified genes (L, M, and H sets containing 1788, 434, and 140 lncRNA genes, respectively) among eight different human cell lines. E, CpG density of promoter regions of m6A-modified genes (L, M, and H sets containing 1074, 290, and 152 lncRNA genes, respectively) among eleven different mouse tissues. F, CpG density of promoter regions of m6A-modified genes (L, M, and H sets containing 618, 120, and 33 lncRNA genes, respectively) among six different mouse cell lines. Significance was evaluated by the two-sided Mann-Whitney test.

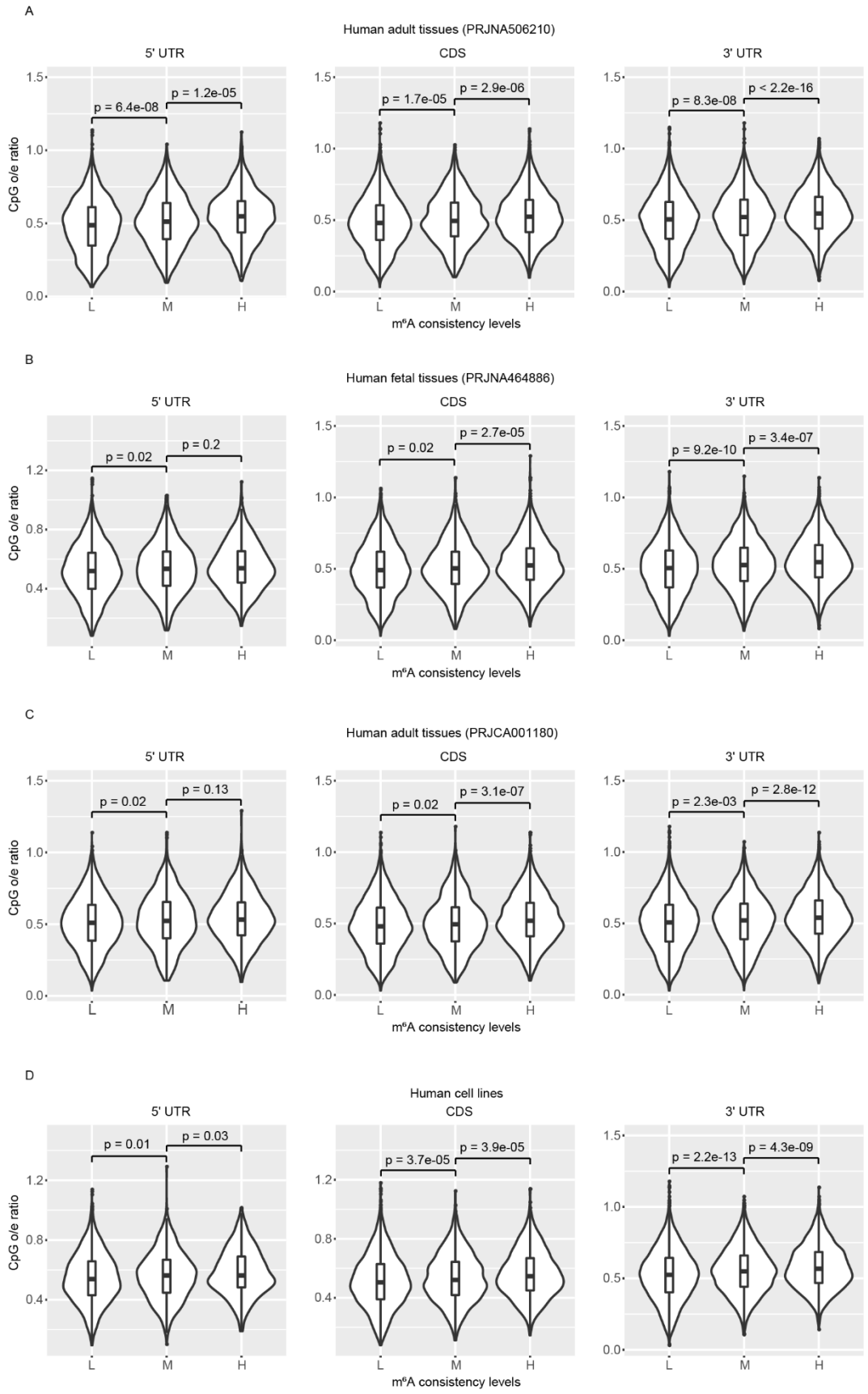

Supplementary Figure 33 **Consistency levels of m6A sites in the mRNA 5'-UTR, CDS, and 3'-UTR positively correlated with the CpG density of the mRNA gene promoter**

region. A, CpG density of promoter regions of m6A-modified genes (for 5'-UTR, L, M, and H sets containing 5124, 1257, and 969 mRNA genes, respectively; for CDS, L, M, and H sets containing 5561, 1746, and 1925 mRNA genes, respectively; for 3'-UTR, L, M, and H sets containing 8060, 3894, and 5916 mRNA genes, respectively) among eight different adult tissues. B, CpG density of promoter regions of m6A-modified genes (for 5'-UTR, L, M, and H sets containing 3522, 1005, and 854 mRNA genes, respectively; for CDS, L, M, and H sets containing 3562, 1398, and 1783 mRNA genes, respectively; for 3'-UTR, L, M, and H sets containing 4744, 2465, and 3742 mRNA genes, respectively) among eight different human fetal tissues. C, CpG density of promoter regions of m6A-modified genes (for 5'-UTR, L, M, and H sets containing 3219, 1017, and 841 mRNA genes, respectively; for CDS, L, M, and H sets containing 4615, 1603, and 2143 mRNA genes, respectively; for 3'-UTR, L, M, and H sets containing 6916, 3275, and 5311 mRNA genes, respectively) among fourteen different adult tissues. D, CpG density of promoter regions of m6A-modified genes (for 5'-UTR, L, M, and H sets containing 3699, 780, and 483 mRNA genes, respectively; for CDS, L, M, and H sets containing 4199, 1536, and 1235 mRNA genes, respectively; for 3'-UTR, L, M, and H sets containing 6276, 3253, and 3468 mRNA genes, respectively) among eight different human cell lines. Significance was evaluated by the two-sided Mann-Whitney test.

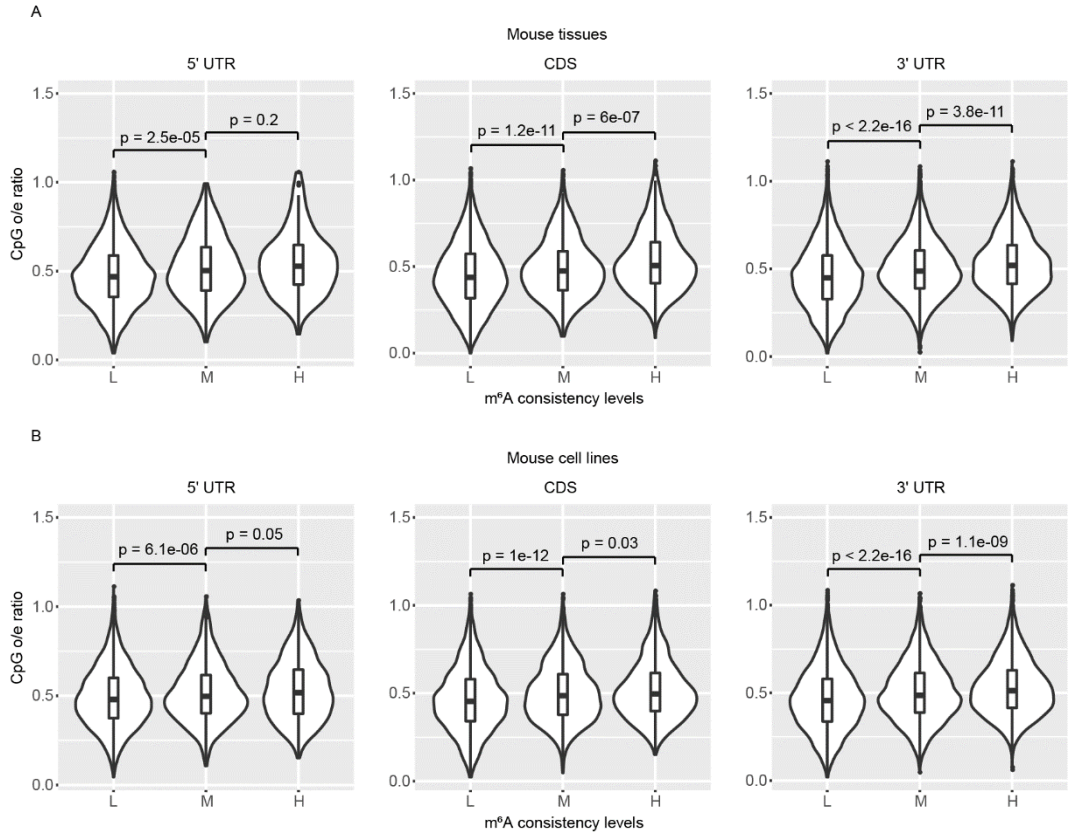

Supplementary Figure 34 **Consistency levels of m6A sites in the mRNA 5'-UTR, CDS, and 3'-UTR positively correlated with the CpG density of the mRNA gene promoter region.** A, CpG density of promoter regions of m6A-modified genes (for 5'-UTR, L, M, and H sets containing 4844, 325, and 144 mRNA genes, respectively; for CDS, L, M, and H sets containing 5923, 1258, and 756 mRNA genes, respectively; for 3'-UTR, L, M, and H sets containing 9445, 2776, and 2273 mRNA genes, respectively) among eleven different mouse tissues. B, CpG density of promoter regions of m6A-modified genes (for 5'-UTR, L, M, and H sets containing 5185, 1432, and 656 mRNA genes, respectively; for CDS, L, M, and H sets containing 4723, 1525, and 1376 mRNA genes, respectively; for 3'-UTR, L, M, and H sets containing 5902, 2801, and 3318 mRNA genes, respectively) among six different mouse cell lines. Significance was evaluated by the two-sided Mann-Whitney test.

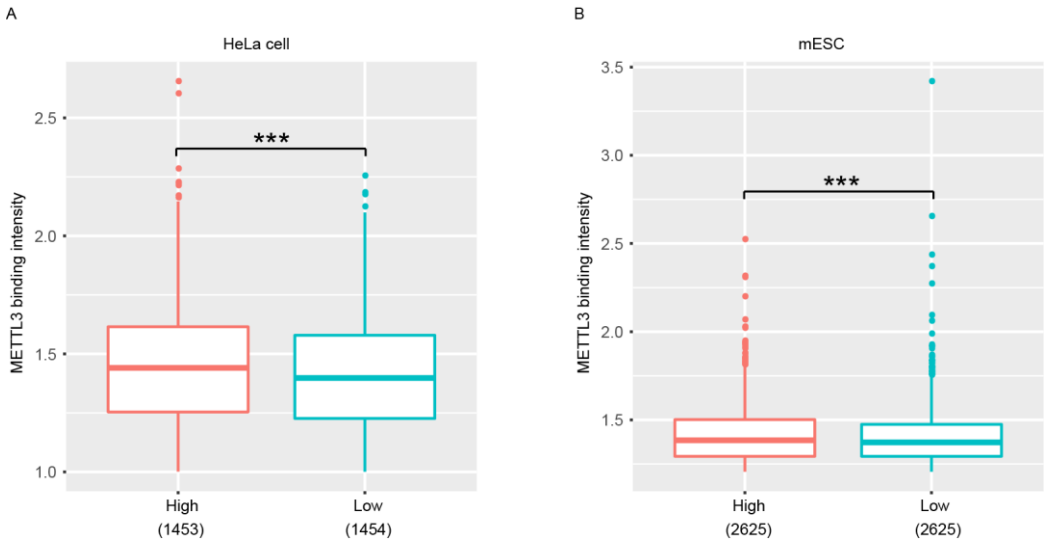

Supplementary Figure 35 **Binding intensity of METTL3 on High-CpG and Low-CpG gene promoter regions.** A, In HeLa, 2907 METTL3-binding genes were classified into two categories, and METTL3 binding intensity was shown. B, In mESC, 5250 METTL3-binding genes were classified into two categories, and METTL3 binding intensity was shown. Significance was evaluated by the two-sided Mann-Whitney test. An asterisk (*) denoted that the P value was between 0.01 and 0.05; Two asterisks (**) denoted that the P value was less than 0.01; Three asterisks (***) denoted that the P value was less than 0.001. NS denoted no significant difference. The numbers in parentheses denoted the number of genes.

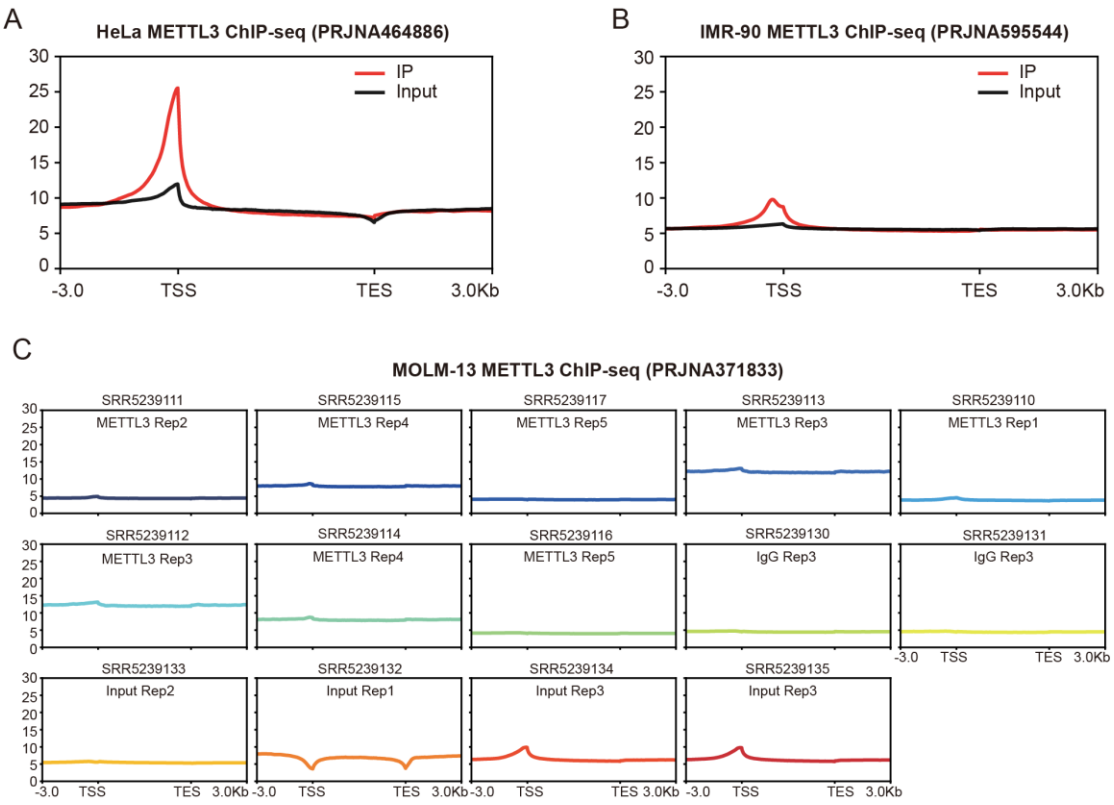

Supplementary Figure 36 **Quality control of METTL3 ChIP-seq data**. A-C, Distribution patterns of METTL3 ChIP-seq reads signals around genes and their 3kb upstream and downstream regions in HeLa (A), IMR-90 (B), and MOLM-13 (C) cell lines.

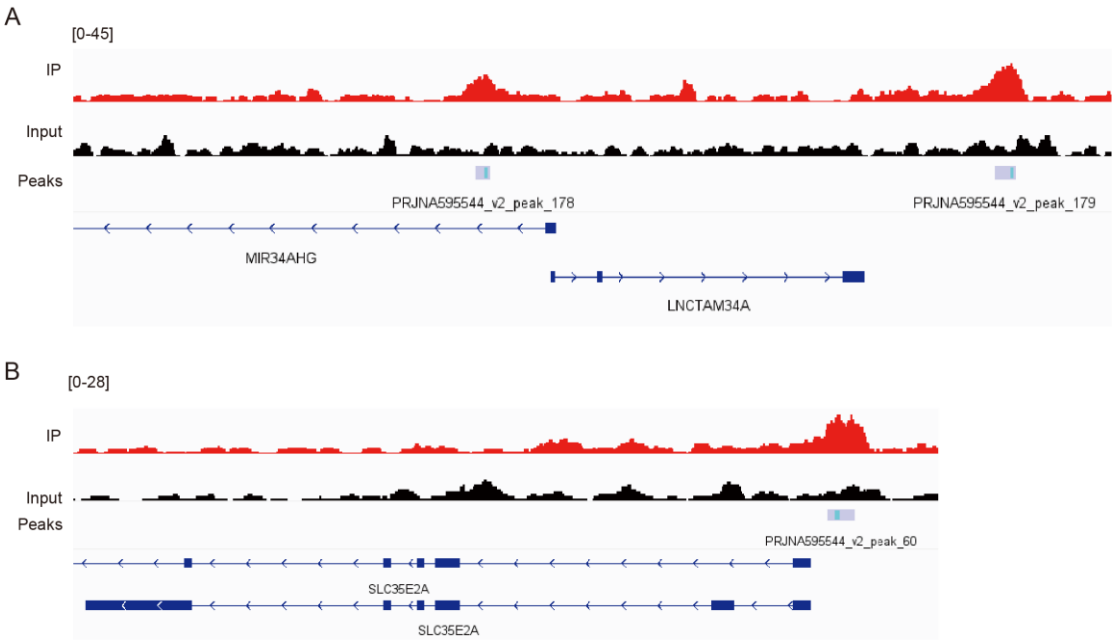

Supplementary Figure 37 IGV examination of METTL3 ChIP-seq read signals in the IMR-90 cell line on the genes *MIR34AHG* (A) and *SLC35E2A* (B). Peaks detected by Macs2 are also displayed.

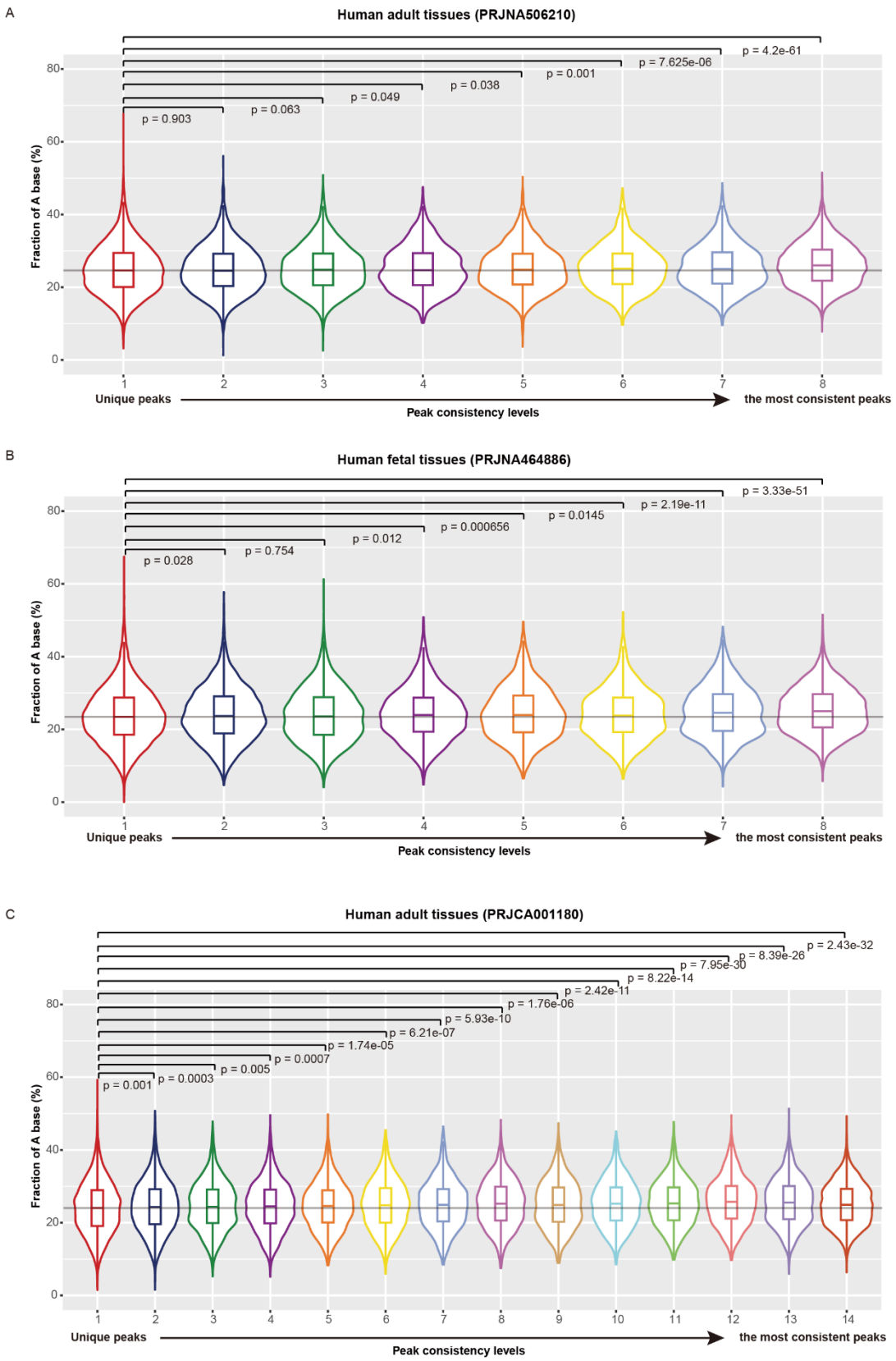

Supplementary Figure 38 The proportion of adenine at m6A sites with different consistency levels. For 8 adult tissues (A), 8 fetal tissues (B), and 14 adult tissues (C), the proportion of adenine at m6A sites with different consistency levels is shown. Significance was evaluated by the two-sided Mann-Whitney test.

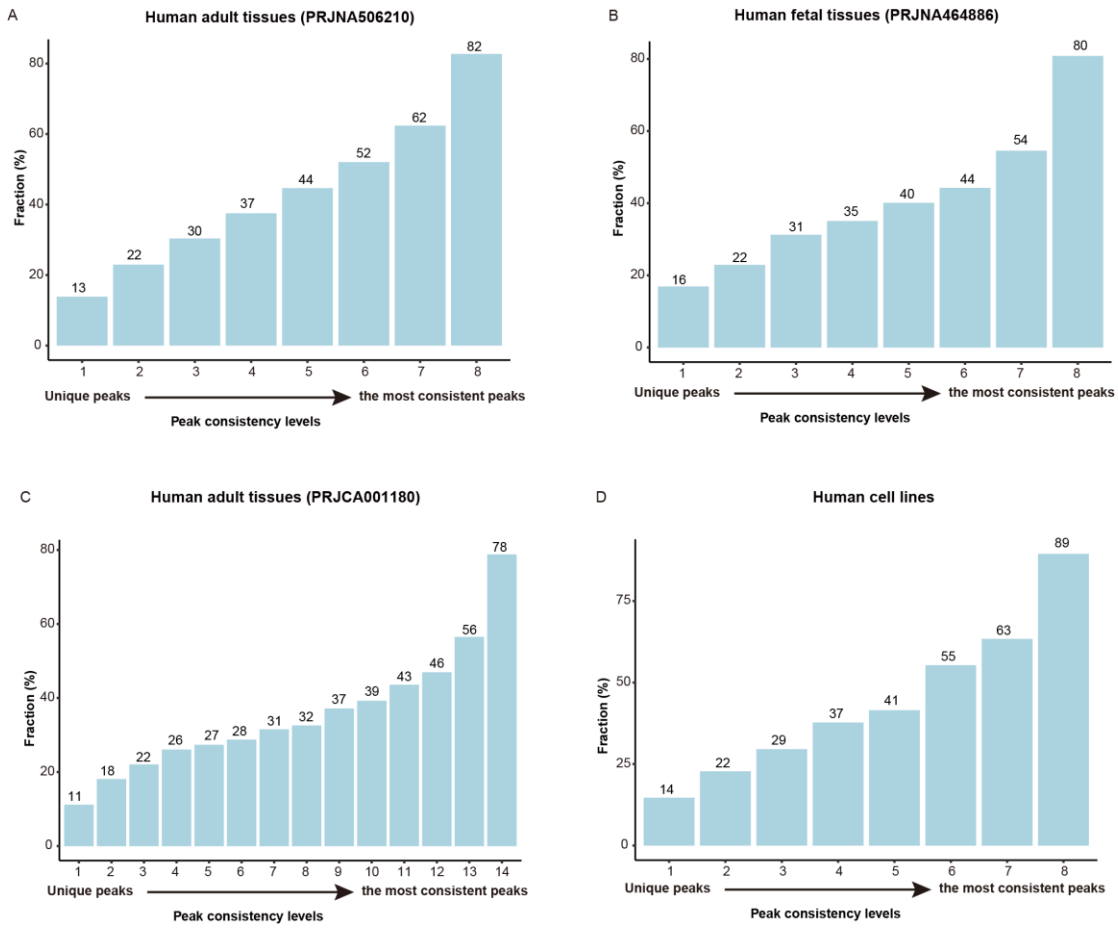

Supplementary Figure 39 Cross-validation of m6A site at different consistency levels using GLORI single-base data in HeLa. The overlap proportions of m6A sites at different consistency levels are shown for 8 adult tissues (A), 8 fetal tissues (B), 14 adult tissues (C), and 8 human cell lines (D).

Supplementary Table 1 m6A-seq data information for different human cell lines

run accession	sample title	library layout	sample type	study accession	antibody info
SRR4310464	GSC-11-rep1	SINGLE	input	PRJNA345000	SYSY
SRR4310465	GSC-11-rep2	SINGLE	input	PRJNA345000	SYSY
SRR4310468	GSC-11-rep1	SINGLE	ip	PRJNA345000	SYSY
SRR4310469	GSC-11-rep2	SINGLE	ip	PRJNA345000	SYSY
SRR3066066	Mono-mac6-rep1	SINGLE	input	PRJNA307239	SYSY
SRR3066067	Mono-mac6-rep1	SINGLE	ip	PRJNA307239	SYSY
SRR3066068	Mono-mac6-rep2	SINGLE	input	PRJNA307239	SYSY
SRR3066069	Mono-mac6-rep2	SINGLE	ip	PRJNA307239	SYSY
SRR5128023	U2OS-rep1	SINGLE	input	PRJNA358676	SYSY
SRR5128024	U2OS-rep1	SINGLE	ip	PRJNA358676	SYSY
SRR5128025	U2OS-rep2	SINGLE	input	PRJNA358676	SYSY
SRR5128026	U2OS-rep2	SINGLE	ip	PRJNA358676	SYSY
SRR5128027	U2OS-rep3	SINGLE	input	PRJNA358676	SYSY
SRR5128028	U2OS-rep3	SINGLE	ip	PRJNA358676	SYSY
SRR494613	HEK293T-rep1	SINGLE	input	PRJNA141085	SYSY
SRR494614	HEK293T-rep1	SINGLE	ip	PRJNA141085	SYSY
SRR494615	HEK293T-rep2	SINGLE	input	PRJNA141085	SYSY
SRR494616	HEK293T-rep2	SINGLE	ip	PRJNA141085	SYSY
SRR494617	HEK293T-rep3	SINGLE	input	PRJNA141085	NEB
SRR494618	HEK293T-rep3	SINGLE	ip	PRJNA141085	NEB

SRR847358	HeLa-rep1	SINGLE	input	PRJNA202057	SYSY
SRR847359	HeLa-rep2	SINGLE	input	PRJNA202057	SYSY
SRR847360	HeLa-rep1	SINGLE	ip	PRJNA202057	SYSY
SRR847361	HeLa-rep2	SINGLE	ip	PRJNA202057	SYSY
SRR847370	HeLa-rep1	SINGLE	input	PRJNA202057	SYSY
SRR847371	HeLa-rep2	SINGLE	input	PRJNA202057	SYSY
SRR847372	HeLa-rep1	SINGLE	ip	PRJNA202057	SYSY
SRR847373	HeLa-rep2	SINGLE	ip	PRJNA202057	SYSY
SRR1035213	hESC-rep1	SINGLE	input	PRJNA229454	SYSY
SRR1035214	hESC-rep1	SINGLE	ip	PRJNA229454	SYSY
SRR1035215	hESC-rep2	SINGLE	input	PRJNA229454	SYSY
SRR1035216	hESC-rep2	SINGLE	ip	PRJNA229454	SYSY
SRR1035221	hESC-rep1	SINGLE	input	PRJNA229454	SYSY
SRR1035222	hESC-rep1	SINGLE	ip	PRJNA229454	SYSY
SRR1035223	hESC-rep2	SINGLE	input	PRJNA229454	SYSY
SRR1035224	hESC-rep2	SINGLE	ip	PRJNA229454	SYSY
SRR1035217	Endoderm-cells-rep1	SINGLE	input	PRJNA229454	SYSY
SRR1035218	Endoderm-cells-rep1	SINGLE	ip	PRJNA229454	SYSY
SRR1035219	Endoderm-cells-rep2	SINGLE	input	PRJNA229454	SYSY
SRR1035220	Endoderm-cells-rep2	SINGLE	ip	PRJNA229454	SYSY
SRR5239086	MOLM13-rep1	SINGLE	input	PRJNA371833	Millipore
SRR5239087	MOLM13-rep1	SINGLE	input	PRJNA371833	Millipore

SRR5239088	MOLM13-rep2	SINGLE	input	PRJNA371833	Millipore
SRR5239089	MOLM13-rep2	SINGLE	input	PRJNA371833	Millipore
SRR5239098	MOLM13-rep1	SINGLE	ip	PRJNA371833	Millipore
SRR5239099	MOLM13-rep1	SINGLE	ip	PRJNA371833	Millipore
SRR5239100	MOLM13-rep2	SINGLE	ip	PRJNA371833	Millipore
SRR5239101	MOLM13-rep2	SINGLE	ip	PRJNA371833	Millipore
SRR2648293	MT4-rep1	SINGLE	input	PRJNA298743	SYSY
SRR2648294	MT4-rep1	SINGLE	ip	PRJNA298743	SYSY
SRR2648296	MT4-rep2	SINGLE	input	PRJNA298743	SYSY
SRR2648297	MT4-rep2	SINGLE	ip	PRJNA298743	SYSY
SRR5931733	HepG2-rep1	SINGLE	input	PRJNA398233	SYSY
SRR5931734	HepG2-rep1	SINGLE	ip	PRJNA398233	SYSY
SRR5931735	HepG2-rep2	SINGLE	input	PRJNA398233	SYSY
SRR5931736	HepG2-rep2	SINGLE	ip	PRJNA398233	SYSY
SRR7992454	NHDF-rep2	SINGLE	ip	PRJNA451188	NEB
SRR7992455	NHDF-rep1	SINGLE	ip	PRJNA451188	NEB
SRR7992458	NHDF-rep1	SINGLE	input	PRJNA451188	NEB
SRR7992459	NHDF-rep3	SINGLE	ip	PRJNA451188	NEB
SRR7992460	NHDF-rep3	SINGLE	input	PRJNA451188	NEB
SRR7992461	NHDF-rep2	SINGLE	input	PRJNA451188	NEB
SRR4310472	HEK293T-rep1	SINGLE	input	PRJNA344999	SYSY
SRR4310473	HEK293T-rep2	SINGLE	input	PRJNA344999	SYSY

SRR4310474	HEK293T-rep3	SINGLE	input	PRJNA344999	SYSY
SRR4310478	HEK293T-rep1	SINGLE	ip	PRJNA344999	SYSY
SRR4310479	HEK293T-rep2	SINGLE	ip	PRJNA344999	SYSY
SRR4310480	HEK293T-rep3	SINGLE	ip	PRJNA344999	SYSY
SRR4042257	Jurkat-rep1	SINGLE	input	PRJNA339176	SYSY
SRR4042258	Jurkat-rep2	SINGLE	input	PRJNA339176	SYSY
SRR4042263	Jurkat-rep1	SINGLE	ip	PRJNA339176	SYSY
SRR4042264	Jurkat-rep2	SINGLE	ip	PRJNA339176	SYSY
SRR903368	U2OS-rep1	SINGLE	input	PRJNA208737	SYSY
SRR903369	U2OS-rep2	SINGLE	input	PRJNA208737	SYSY
SRR903370	U2OS-rep3	SINGLE	input	PRJNA208737	SYSY
SRR903374	U2OS-rep1	SINGLE	ip	PRJNA208737	SYSY
SRR903375	U2OS-rep2	SINGLE	ip	PRJNA208737	SYSY
SRR903376	U2OS-rep3	SINGLE	ip	PRJNA208737	SYSY
SRR456551	HepG2-rep1	SINGLE	ip	PRJNA158111	SYSY
SRR456552	HepG2-rep2	SINGLE	ip	PRJNA158111	SYSY
SRR456553	HepG2-rep3	SINGLE	ip	PRJNA158111	SYSY
SRR456555	HepG2-rep1	SINGLE	input	PRJNA158111	SYSY
SRR456556	HepG2-rep2	SINGLE	input	PRJNA158111	SYSY
SRR456557	HepG2-rep3	SINGLE	input	PRJNA158111	SYSY
SRR5925271	HeLa-rep1	PAIRED	input	PRJNA397879	SYSY
SRR5925272	HeLa-rep2	PAIRED	input	PRJNA397879	SYSY
SRR5925273	HeLa-rep1	PAIRED	ip	PRJNA397879	SYSY
SRR5925274	HeLa-rep2	PAIRED	ip	PRJNA397879	SYSY
SRR6686554	HepG2-rep1	SINGLE	input	PRJNA433472	SYSY

SRR6686555	HepG2-rep2	SINGLE	input	PRJNA433472	SYSY
SRR6686556	HepG2-rep3	SINGLE	input	PRJNA433472	SYSY
SRR6686557	HepG2-rep1	SINGLE	ip	PRJNA433472	SYSY
SRR6686558	HepG2-rep2	SINGLE	ip	PRJNA433472	SYSY
SRR6686559	HepG2-rep3	SINGLE	ip	PRJNA433472	SYSY
SRR6954135	HeLa-rep1	SINGLE	input	PRJNA448996	SYSY
SRR6954136	HeLa-rep2	SINGLE	input	PRJNA448996	SYSY
SRR6954137	HeLa-rep1	SINGLE	ip	PRJNA448996	SYSY
SRR6954138	HeLa-rep2	SINGLE	ip	PRJNA448996	SYSY
SRR14765588	HEK293T-rep1	PAIRED	input	PRJNA634388	SYSY
SRR14765589	HEK293T-rep1	PAIRED	ip	PRJNA634388	SYSY
SRR14765590	HEK293T-rep2	PAIRED	input	PRJNA634388	SYSY
SRR14765591	HEK293T-rep2	PAIRED	ip	PRJNA634388	SYSY
2020082301	hESC-rep1	PAIRED	input	PRJNA665206	NEB
2020082303	hESC-rep1	PAIRED	ip	PRJNA665206	NEB
2020082305	hESC-rep2	PAIRED	input	PRJNA665206	NEB
2020082307	hESC-rep2	PAIRED	ip	PRJNA665206	NEB
CRR072994	HeLa-rep1	PAIRED	input	PRJCA001180	Millipore
CRR072995	HeLa-rep1	PAIRED	ip	PRJCA001180	Millipore
CRR072996	HeLa-rep2	PAIRED	input	PRJCA001180	Millipore
CRR072997	HeLa-rep2	PAIRED	ip	PRJCA001180	Millipore
CRR073001	K562-rep1	PAIRED	ip	PRJCA001180	Millipore

CRR073003	K562-rep2	PAIRED	ip	PRJCA001180	Millipore
CRR073000	K562-rep1	PAIRED	input	PRJCA001180	Millipore
CRR073002	K562-rep2	PAIRED	input	PRJCA001180	Millipore
CRR073007	WPMY-rep1	PAIRED	ip	PRJCA001180	Millipore
CRR073009	WPMY-rep2	PAIRED	ip	PRJCA001180	Millipore
CRR073006	WPMY-rep1	PAIRED	input	PRJCA001180	Millipore
CRR073008	WPMY-rep2	PAIRED	input	PRJCA001180	Millipore
CRR073013	Jurkat-rep1	PAIRED	ip	PRJCA001180	Millipore
CRR073015	Jurkat-rep2	PAIRED	ip	PRJCA001180	Millipore
CRR073012	Jurkat-rep1	PAIRED	input	PRJCA001180	Millipore
CRR073014	Jurkat-rep2	PAIRED	input	PRJCA001180	Millipore
CRR042274	HEK293T-rep1	PAIRED	ip	PRJCA001180	Millipore
CRR042276	HEK293T-rep2	PAIRED	ip	PRJCA001180	Millipore
CRR055565	HEK293T-rep3	PAIRED	ip	PRJCA001180	Millipore
CRR042275	HEK293T-rep1	PAIRED	input	PRJCA001180	Millipore
CRR042277	HEK293T-rep2	PAIRED	input	PRJCA001180	Millipore
CRR055566	HEK293T-rep3	PAIRED	input	PRJCA001180	Millipore

Supplementary Table 2 m6A-seq data information for different human tissues

Run accession	Sample title	Library layout	Sample type	Study accession	Antibody info
CRR042290	Heart-4-2	PAIRED	ip	PRJCA001180	Millipore
CRR042291	Heart-4-2	PAIRED	input	PRJCA001180	Millipore
CRR055527	Heart-1-1	PAIRED	ip	PRJCA001180	Millipore
CRR055528	Heart-1-1	PAIRED	input	PRJCA001180	Millipore
CRR042302	Skin-4-2	PAIRED	ip	PRJCA001180	Millipore
CRR042303	Skin-4-2	PAIRED	input	PRJCA001180	Millipore
CRR042304	Skin-1-1	PAIRED	ip	PRJCA001180	Millipore
CRR042305	Skin-1-1	PAIRED	input	PRJCA001180	Millipore
CRR042284	Cerebellum-5-3	PAIRED	ip	PRJCA001180	Millipore
CRR073016	Cerebellum-7-4	PAIRED	ip	PRJCA001180	Millipore
CRR042285	Cerebellum-5-3	PAIRED	input	PRJCA001180	Millipore
CRR073017	Cerebellum-7-4	PAIRED	input	PRJCA001180	Millipore
CRR042286	Cerebrum-5-3	PAIRED	ip	PRJCA001180	Millipore
CRR055553	Cerebrum-6-3	PAIRED	ip	PRJCA001180	Millipore
CRR042287	Cerebrum-5-3	PAIRED	input	PRJCA001180	Millipore
CRR055554	Cerebrum-6-3	PAIRED	input	PRJCA001180	Millipore
CRR042312	Thyroid-gland-4-2	PAIRED	ip	PRJCA001180	Millipore
CRR042314	Thyroid-gland-5-3	PAIRED	ip	PRJCA001180	Millipore
CRR042313	Thyroid-gland-4-2	PAIRED	input	PRJCA001180	Millipore
CRR042315	Thyroid-gland-5-3	PAIRED	input	PRJCA001180	Millipore
CRR042306	Stomach-4-2	PAIRED	ip	PRJCA001180	Millipore
CRR042308	Stomach-5-3	PAIRED	ip	PRJCA001180	Millipore
CRR042307	Stomach-4-2	PAIRED	input	PRJCA001180	Millipore
CRR042309	Stomach-5-3	PAIRED	input	PRJCA001180	Millipore
CRR055551	Jejunum-4-2	PAIRED	ip	PRJCA001180	Millipore
CRR055555	Jejunum-5-3	PAIRED	ip	PRJCA001180	Millipore
CRR055552	Jejunum-4-2	PAIRED	input	PRJCA001180	Millipore
CRR055556	Jejunum-5-3	PAIRED	input	PRJCA001180	Millipore
CRR055543	Appendix-3-2	PAIRED	ip	PRJCA001180	Millipore
CRR055557	Appendix-5-3	PAIRED	ip	PRJCA001180	Millipore
CRR055544	Appendix-3-2	PAIRED	input	PRJCA001180	Millipore
CRR055558	Appendix-5-3	PAIRED	input	PRJCA001180	Millipore
CRR055559	Rectum-5-3	PAIRED	ip	PRJCA001180	Millipore
CRR055563	Rectum-4-2	PAIRED	ip	PRJCA001180	Millipore
CRR055560	Rectum-5-3	PAIRED	input	PRJCA001180	Millipore
CRR055564	Rectum-4-2	PAIRED	input	PRJCA001180	Millipore
CRR042280	Aorta-4-2	PAIRED	ip	PRJCA001180	Millipore
CRR055531	Aorta-1-1	PAIRED	ip	PRJCA001180	Millipore
CRR042281	Aorta-4-2	PAIRED	input	PRJCA001180	Millipore
CRR055532	Aorta-1-1	PAIRED	input	PRJCA001180	Millipore
CRR055547	Esophagus-3-2	PAIRED	ip	PRJCA001180	Millipore

CRR055561	Esophagus-4-2	PAIRED	ip	PRJCA001180	Millipore
CRR055548	Esophagus-3-2	PAIRED	input	PRJCA001180	Millipore
CRR055562	Esophagus-4-2	PAIRED	input	PRJCA001180	Millipore
CRR055529	Spleen-1-1	PAIRED	ip	PRJCA001180	Millipore
CRR055536	Spleen-2-1	PAIRED	ip	PRJCA001180	Millipore
CRR055541	Spleen-3-2	PAIRED	ip	PRJCA001180	Millipore
CRR055530	Spleen-1-1	PAIRED	input	PRJCA001180	Millipore
CRR055535	Spleen-2-1	PAIRED	input	PRJCA001180	Millipore
CRR055542	Spleen-3-2	PAIRED	input	PRJCA001180	Millipore
CRR042318	Urinary-bladder-4-2	PAIRED	ip	PRJCA001180	Millipore
CRR042320	Urinary-bladder-5-3	PAIRED	ip	PRJCA001180	Millipore
CRR055539	Urinary-bladder-2-1	PAIRED	ip	PRJCA001180	Millipore
CRR042319	Urinary-bladder-4-2	PAIRED	input	PRJCA001180	Millipore
CRR042321	Urinary-bladder-5-3	PAIRED	input	PRJCA001180	Millipore
CRR055540	Urinary-bladder-2-1	PAIRED	input	PRJCA001180	Millipore
CRR042296	Lung-4-2	PAIRED	ip	PRJCA001180	Millipore
CRR055533	Lung-2-1	PAIRED	ip	PRJCA001180	Millipore
CRR073018	Lung-2-4	PAIRED	ip	PRJCA001180	Millipore
CRR073020	Lung-4-4	PAIRED	ip	PRJCA001180	Millipore
CRR042297	Lung-4-2	PAIRED	input	PRJCA001180	Millipore
CRR055534	Lung-2-1	PAIRED	input	PRJCA001180	Millipore
CRR073019	Lung-2-4	PAIRED	input	PRJCA001180	Millipore
CRR073021	Lung-4-4	PAIRED	input	PRJCA001180	Millipore
SRR8209837	Cerebellum-1	PAIRED	ip	PRJNA506210	SYSY
SRR8209839	Cerebellum-2	PAIRED	ip	PRJNA506210	SYSY
SRR8209841	Cerebellum-3	PAIRED	ip	PRJNA506210	SYSY
SRR8209836	Cerebellum-1	PAIRED	input	PRJNA506210	SYSY
SRR8209838	Cerebellum-2	PAIRED	input	PRJNA506210	SYSY
SRR8209840	Cerebellum-3	PAIRED	input	PRJNA506210	SYSY
SRR8209843	FrontalCortex-1	PAIRED	ip	PRJNA506210	SYSY
SRR8209845	FrontalCortex-2	PAIRED	ip	PRJNA506210	SYSY
SRR8209847	FrontalCortex-3	PAIRED	ip	PRJNA506210	SYSY
SRR8209842	FrontalCortex-1	PAIRED	input	PRJNA506210	SYSY
SRR820984	FrontalCortex-2	PAIRED	input	PRJNA50621	SYSY

4				0	
SRR820984	FrontalCortex-3	PAIRED	input	PRJNA50621	SYSY
6				0	
SRR820984	Heart-1	PAIRED	ip	PRJNA50621	SYSY
9				0	
SRR820985	Heart-2	PAIRED	ip	PRJNA50621	SYSY
3				0	
SRR820985	Heart-3	PAIRED	ip	PRJNA50621	SYSY
5				0	
SRR820984	Heart-1	PAIRED	input	PRJNA50621	SYSY
8				0	
SRR820985	Heart-2	PAIRED	input	PRJNA50621	SYSY
0				0	
SRR820985	Heart-3	PAIRED	input	PRJNA50621	SYSY
4				0	
SRR820985	Kidney-1	PAIRED	ip	PRJNA50621	SYSY
7				0	
SRR820985	Kidney-2	PAIRED	ip	PRJNA50621	SYSY
9				0	
SRR820986	Kidney-3	PAIRED	ip	PRJNA50621	SYSY
1				0	
SRR820985	Kidney-1	PAIRED	input	PRJNA50621	SYSY
6				0	
SRR820985	Kidney-2	PAIRED	input	PRJNA50621	SYSY
8				0	
SRR820986	Kidney-3	PAIRED	input	PRJNA50621	SYSY
0				0	
SRR820986	Liver-1	PAIRED	ip	PRJNA50621	SYSY
3				0	
SRR820986	Liver-2	PAIRED	ip	PRJNA50621	SYSY
5				0	
SRR820986	Liver-3	PAIRED	ip	PRJNA50621	SYSY
7				0	
SRR820986	Liver-1	PAIRED	input	PRJNA50621	SYSY
2				0	
SRR820986	Liver-2	PAIRED	input	PRJNA50621	SYSY
4				0	
SRR820986	Liver-3	PAIRED	input	PRJNA50621	SYSY
6				0	
SRR820986	Lung-1	PAIRED	ip	PRJNA50621	SYSY
9				0	
SRR820987	Lung-2	PAIRED	ip	PRJNA50621	SYSY
1				0	
SRR820987	Lung-3	PAIRED	ip	PRJNA50621	SYSY

3				0	
SRR820986	Lung-1	PAIRED	input	PRJNA50621	SYSY
8				0	
SRR820987	Lung-2	PAIRED	input	PRJNA50621	SYSY
0				0	
SRR820987	Lung-3	PAIRED	input	PRJNA50621	SYSY
2				0	
SRR820987	Muscle-1	PAIRED	ip	PRJNA50621	SYSY
5				0	
SRR820987	Muscle-2	PAIRED	ip	PRJNA50621	SYSY
7				0	
SRR820987	Muscle-3	PAIRED	ip	PRJNA50621	SYSY
9				0	
SRR820987	Muscle-1	PAIRED	input	PRJNA50621	SYSY
4				0	
SRR820987	Muscle-2	PAIRED	input	PRJNA50621	SYSY
6				0	
SRR820987	Muscle-3	PAIRED	input	PRJNA50621	SYSY
8				0	
SRR820988	Spleen-1	PAIRED	ip	PRJNA50621	SYSY
1				0	
SRR820988	Spleen-2	PAIRED	ip	PRJNA50621	SYSY
3				0	
SRR820988	Spleen-3	PAIRED	ip	PRJNA50621	SYSY
5				0	
SRR820988	Spleen-1	PAIRED	input	PRJNA50621	SYSY
0				0	
SRR820988	Spleen-2	PAIRED	input	PRJNA50621	SYSY
2				0	
SRR820988	Spleen-3	PAIRED	input	PRJNA50621	SYSY
4				0	
SRR713085	heart-1	SINGLE	ip	PRJNA46488	Abcam
7				6	
SRR713085	heart-2	SINGLE	ip	PRJNA46488	Abcam
8				6	
SRR713085	heart-3	SINGLE	ip	PRJNA46488	Abcam
9				6	
SRR713087	heart-1	PAIRED	input	PRJNA46488	Abcam
9				6	
SRR713088	heart-2	PAIRED	input	PRJNA46488	Abcam
0				6	
SRR713088	heart-3	PAIRED	input	PRJNA46488	Abcam
1				6	
SRR713086	kidney-2	SINGLE	ip	PRJNA46488	Abcam

0				6	
SRR713086	kidney-3	SINGLE	ip	PRJNA46488	Abcam
1				6	
SRR713086	kidney-4	SINGLE	ip	PRJNA46488	Abcam
2				6	
SRR713088	kidney-2	PAIRED	input	PRJNA46488	Abcam
2				6	
SRR713088	kidney-3	PAIRED	input	PRJNA46488	Abcam
3				6	
SRR713088	kidney-4	PAIRED	input	PRJNA46488	Abcam
4				6	
SRR713086	liver-1	SINGLE	ip	PRJNA46488	Abcam
3				6	
SRR713086	liver-2	SINGLE	ip	PRJNA46488	Abcam
4				6	
SRR713086	liver-3	SINGLE	ip	PRJNA46488	Abcam
5				6	
SRR713088	liver-1	PAIRED	input	PRJNA46488	Abcam
5				6	
SRR713088	liver-2	PAIRED	input	PRJNA46488	Abcam
6				6	
SRR713088	liver-3	PAIRED	input	PRJNA46488	Abcam
7				6	
SRR713087	placenta-2	SINGLE	ip	PRJNA46488	Abcam
2				6	
SRR713087	placenta-4	SINGLE	ip	PRJNA46488	Abcam
3				6	
SRR713087	placenta-6	SINGLE	ip	PRJNA46488	Abcam
4				6	
SRR713089	placenta-2	PAIRED	input	PRJNA46488	Abcam
4				6	
SRR713089	placenta-4	PAIRED	input	PRJNA46488	Abcam
5				6	
SRR713089	placenta-6	PAIRED	input	PRJNA46488	Abcam
6				6	
SRR713086	lung-4	SINGLE	ip	PRJNA46488	Abcam
6				6	
SRR713086	lung-5	SINGLE	ip	PRJNA46488	Abcam
7				6	
SRR713088	lung-4	PAIRED	input	PRJNA46488	Abcam
8				6	
SRR713088	lung-5	PAIRED	input	PRJNA46488	Abcam
9				6	
SRR713086	muscle-4	SINGLE	ip	PRJNA46488	Abcam

8				6	
SRR7130869	muscle-5	SINGLE	ip	PRJNA464886	Abcam
SRR7130890	muscle-4	PAIRED	input	PRJNA464886	Abcam
SRR7130891	muscle-5	PAIRED	input	PRJNA464886	Abcam
SRR7130870	stomach-4	SINGLE	ip	PRJNA464886	Abcam
SRR7130871	stomach-5	SINGLE	ip	PRJNA464886	Abcam
SRR7130892	stomach-4	PAIRED	input	PRJNA464886	Abcam
SRR7130893	stomach-5	PAIRED	input	PRJNA464886	Abcam
SRR7130854	brain-1	SINGLE	ip	PRJNA464886	Abcam
SRR7130855	brain-2	SINGLE	ip	PRJNA464886	Abcam
SRR7130856	brain-3	SINGLE	ip	PRJNA464886	Abcam
SRR7130875	brain-1	PAIRED	input	PRJNA464886	Abcam
SRR7130876	brain-2	PAIRED	input	PRJNA464886	Abcam
SRR7130877	brain-3	PAIRED	input	PRJNA464886	Abcam
SRR7130878	brain-4	PAIRED	input	PRJNA464886	Abcam

Supplementary Table 3 m6A-seq data information for different mouse cell lines

run accession	sample title	library layout	sample type	study accession	antibody info
SRR6144434	NPC-rep1	SINGLE	input	PRJNA413499	SYSY
SRR6144435	NPC-rep2	SINGLE	input	PRJNA413499	SYSY
SRR6144436	NPC-rep1	SINGLE	ip	PRJNA413499	SYSY
SRR6144437	NPC-rep2	SINGLE	ip	PRJNA413499	SYSY
SRR1596085	mESC-rep1	SINGLE	ip	PRJNA262906	SYSY
SRR1596086	mESC-rep1	SINGLE	input	PRJNA262906	SYSY
SRR1596087	mESC-rep2	SINGLE	ip	PRJNA262906	SYSY
SRR1596088	mESC-rep2	SINGLE	input	PRJNA262906	SYSY
SRR1596089	mESC-rep3	SINGLE	ip	PRJNA262906	SYSY
SRR1596090	mESC-rep3	SINGLE	input	PRJNA262906	SYSY
SRR1596097	MEF-rep1	SINGLE	ip	PRJNA262906	SYSY
SRR1596098	MEF-rep1	SINGLE	input	PRJNA262906	SYSY
SRR1596099	MEF-rep2	SINGLE	ip	PRJNA262906	SYSY
SRR1596100	MEF-rep2	SINGLE	input	PRJNA262906	SYSY
SRR1048180	3T3-L1-rep1	SINGLE	input	PRJNA231244	SYSY
SRR1048181	3T3-L1-rep1	SINGLE	ip	PRJNA231244	SYSY
SRR1575981	3T3-L1-rep2	SINGLE	input	PRJNA231244	SYSY
SRR1575982	3T3-L1-rep2	SINGLE	ip	PRJNA231244	SYSY
SRR6163656	NSPC-rep1	SINGLE	input	PRJNA414058	NEB
SRR6163657	NSPC-rep2	SINGLE	input	PRJNA414058	NEB

SRR6163658	NSPC-rep3	SINGLE	input	PRJNA414058	NEB
SRR6163662	NSPC-rep1	SINGLE	ip	PRJNA414058	NEB
SRR6163663	NSPC-rep2	SINGLE	ip	PRJNA414058	NEB
SRR6163664	NSPC-rep3	SINGLE	ip	PRJNA414058	NEB
SRR7235655	Dendritic-cells-rep1	SINGLE	input	PRJNA473808	NEB
SRR7235656	Dendritic-cells-rep2	SINGLE	input	PRJNA473808	NEB
SRR7235659	Dendritic-cells-rep1	SINGLE	ip	PRJNA473808	NEB
SRR7235660	Dendritic-cells-rep2	SINGLE	ip	PRJNA473808	NEB
SRR8130792	Dendritic-cells-rep1	PAIRED	ip	PRJNA499089	NEB
SRR8130793	Dendritic-cells-rep2	PAIRED	ip	PRJNA499089	NEB
SRR8130796	Dendritic-cells-rep1	PAIRED	input	PRJNA499089	NEB
SRR8130797	Dendritic-cells-rep2	PAIRED	input	PRJNA499089	NEB
SRR14765644	mESC-rep1	PAIRED	input	PRJNA634388	NEB
SRR14765645	mESC-rep1	PAIRED	ip	PRJNA634388	NEB
SRR14765646	mESC-rep2	PAIRED	input	PRJNA634388	NEB
SRR14765647	mESC-rep2	PAIRED	ip	PRJNA634388	NEB

Supplementary Table 4 m6A-seq data information for different mouse tissues

run accession	sample title	library layout	sample type	study accession	antibody info
SRR496283	Brain-1	SINGLE	ip	PRJNA141085	SYSY
SRR496284	Brain-1	SINGLE	input	PRJNA141085	SYSY
SRR496285	Brain-2	SINGLE	input	PRJNA141085	SYSY
SRR496287	Brain-2	SINGLE	ip	PRJNA141085	SYSY
SRR1596091	Embryoid-bodies-1	SINGLE	ip	PRJNA262906	SYSY
SRR1596092	Embryoid-bodies-1	SINGLE	input	PRJNA262906	SYSY
SRR1596093	Embryoid-bodies-2	SINGLE	ip	PRJNA262906	SYSY
SRR1596094	Embryoid-bodies-2	SINGLE	input	PRJNA262906	SYSY
SRR1596096	Embryoid-bodies-3	SINGLE	input	PRJNA262906	SYSY
SRR1745915	Embryoid-bodies-3	SINGLE	ip	PRJNA262906	SYSY
SRR5468919	Testis-1	SINGLE	ip	PRJNA383941	SYSY
SRR5468920	Testis-2	SINGLE	ip	PRJNA383941	SYSY
SRR5468921	Testis-1	SINGLE	input	PRJNA383941	SYSY
SRR5468922	Testis-2	SINGLE	input	PRJNA383941	SYSY
SRR866997	Midbrain-1	SINGLE	ip	PRJNA205151	SYSY
SRR866998	Midbrain-1	SINGLE	input	PRJNA205151	SYSY
SRR866999	Midbrain-2	SINGLE	ip	PRJNA205151	SYSY
SRR867000	Midbrain-2	SINGLE	input	PRJNA205151	SYSY
SRR867001	Midbrain-3	SINGLE	ip	PRJNA205151	SYSY
SRR867002	Midbrain-3	SINGLE	input	PRJNA205151	SYSY
SRR520481	Hippocampus	SINGL	input	PRJNA36884	SYSY

1	-2-weeks-1	E		9	
SRR520481	Hippocampus	SINGL	input	PRJNA36884	SYSY
2	-2-weeks-2	E		9	
SRR520481	Hippocampus	SINGL	ip	PRJNA36884	SYSY
3	-2-weeks-1	E		9	
SRR520481	Hippocampus	SINGL	ip	PRJNA36884	SYSY
4	-2-weeks-2	E		9	
SRR520481	Hippocampus	SINGL	input	PRJNA36884	SYSY
5	-6-weeks-1	E		9	
SRR520481	Hippocampus	SINGL	input	PRJNA36884	SYSY
6	-6-weeks-2	E		9	
SRR520481	Hippocampus	SINGL	ip	PRJNA36884	SYSY
7	-6-weeks-1	E		9	
SRR520481	Hippocampus	SINGL	ip	PRJNA36884	SYSY
8	-6-weeks-2	E		9	
CRR055567	Heart-1-5	PAIRE	input	PRJCA00118	Millipor
		D		0	e
CRR055568	Heart-1-5	PAIRE	ip	PRJCA00118	Millipor
		D		0	e
CRR072984	Heart-1-4	PAIRE	input	PRJCA00118	Millipor
		D		0	e
CRR072985	Heart-1-4	PAIRE	ip	PRJCA00118	Millipor
		D		0	e
CRR055583	Heart-2-5	PAIRE	input	PRJCA00118	Millipor
		D		0	e
CRR055584	Heart-2-5	PAIRE	ip	PRJCA00118	Millipor
		D		0	e
CRR055569	Spleen-1-5	PAIRE	input	PRJCA00118	Millipor
		D		0	e
CRR055570	Spleen-1-5	PAIRE	ip	PRJCA00118	Millipor
		D		0	e
CRR055585	Spleen-2-5	PAIRE	input	PRJCA00118	Millipor
		D		0	e
CRR055586	Spleen-2-5	PAIRE	ip	PRJCA00118	Millipor
		D		0	e
CRR055573	Liver-1-5	PAIRE	input	PRJCA00118	Millipor
		D		0	e
CRR055574	Liver-1-5	PAIRE	ip	PRJCA00118	Millipor
		D		0	e
CRR072982	Liver-1-4	PAIRE	input	PRJCA00118	Millipor
		D		0	e
CRR072983	Liver-1-4	PAIRE	ip	PRJCA00118	Millipor
		D		0	e
CRR055589	Liver-2-5	PAIRE	input	PRJCA00118	Millipor

		D		0	e
CRR055590	Liver-2-5	PAIRED	ip	PRJCA001180	Millipore
CRR055593	Cerebellum-2-5	PAIRED	input	PRJCA001180	Millipore
CRR055594	Cerebellum-2-5	PAIRED	ip	PRJCA001180	Millipore
CRR055577	Cerebellum-1-5	PAIRED	input	PRJCA001180	Millipore
CRR055578	Cerebellum-1-5	PAIRED	ip	PRJCA001180	Millipore
CRR055581	Hypothalamus-1-5	PAIRED	input	PRJCA001180	Millipore
CRR055582	Hypothalamus-1-5	PAIRED	ip	PRJCA001180	Millipore
CRR055597	Hypothalamus-2-5	PAIRED	input	PRJCA001180	Millipore
CRR055598	Hypothalamus-2-5	PAIRED	ip	PRJCA001180	Millipore
CRR055575	Cerebrum-1-5	PAIRED	input	PRJCA001180	Millipore
CRR055576	Cerebrum-1-5	PAIRED	ip	PRJCA001180	Millipore
CRR055591	Cerebrum-2-5	PAIRED	input	PRJCA001180	Millipore
CRR055592	Cerebrum-2-5	PAIRED	ip	PRJCA001180	Millipore
CRR055579	Brainstem-1-5	PAIRED	input	PRJCA001180	Millipore
CRR055580	Brainstem-1-5	PAIRED	ip	PRJCA001180	Millipore
CRR055595	Brainstem-2-5	PAIRED	input	PRJCA001180	Millipore
CRR055596	Brainstem-2-5	PAIRED	ip	PRJCA001180	Millipore
CRR055587	Lung-2-5	PAIRED	input	PRJCA001180	Millipore
CRR055588	Lung-2-5	PAIRED	ip	PRJCA001180	Millipore
CRR055571	Lung-1-5	PAIRED	input	PRJCA001180	Millipore
CRR055572	Lung-1-5	PAIRED	ip	PRJCA001180	Millipore
CRR072986	Lung-1-4	PAIRE	input	PRJCA00118	Millipor

		D		0	e
CRR072987	Lung-1-4	PAIRE D	ip	PRJCA00118 0	Millipor e
CRR072988	Lung-2-4	PAIRE D	input	PRJCA00118 0	Millipor e
CRR072989	Lung-2-4	PAIRE D	ip	PRJCA00118 0	Millipor e

Supplementary Table 5 ChIP-seq data information for HeLa and mESC

run accession	sample title	library layout	sample type	study accession
SRR7130897	HeLa-METTL3	SINGLE	input	PRJNA464886
SRR7130898	HeLa-METTL3	SINGLE	ip	PRJNA464886
SRR8545657	mESC-METTL3	PAIRED	input	PRJNA521368
SRR12187085	mESC-METTL3-rep1	PAIRED	ip	PRJNA521368
SRR12187193	mESC-METTL3-rep2	PAIRED	ip	PRJNA521368